

1 **Title page**

2

3 **Title:**

4 Context-specific functions of Notch in *Drosophila* blood cell progenitors

5

6 **Running title:**

7 Notch roles in blood cell progenitors

8

9 **Names and affiliations of all authors:**

10 Blanco-Obregon, DM<sup>1\*</sup>; Katz, MJ<sup>1,2\*</sup>; Durrieu, L<sup>1,3</sup>; Gándara, L<sup>1,2</sup>; Wappner, P<sup>1,2,3\*\*</sup>

11 1. Instituto Leloir, CONICET, Patricias Argentinas 435, Buenos Aires (1405), Argentina.

12 2. Consejo Nacional de Investigaciones Científicas y Técnicas (CONICET), Buenos Aires,  
13 Argentina.

14 3. Departamento de Fisiología, Biología Molecular y Celular, Facultad de Ciencias Exactas y  
15 Naturales-Universidad de Buenos Aires, Buenos Aires (1428), Argentina.

16

17 \* Contributed equally to this work.

18 \*\*Corresponding author: [pwappner@leloir.org.ar](mailto:pwappner@leloir.org.ar).

19

20 **Key words:**

21 *Drosophila* hematopoiesis; Blood cell progenitors; Notch signaling; Lymph gland

## 22 **Summary statement**

- 23 Notch signaling regulates differently distinct populations of blood cell progenitors of the  
24 *Drosophila* larval hematopoietic organ.

## 25 **Abstract**

26 *Drosophila* Larval hematopoiesis takes place at the lymph gland, where myeloid-like  
27 progenitors differentiate into Plasmacytes and Crystal Cells, under regulation of conserved  
28 signaling pathways. It has been established that the Notch pathway plays a specific role in  
29 Crystal Cell differentiation and maintenance. In mammalian hematopoiesis, the Notch pathway  
30 has been proposed to fulfill broader functions, including HSCs maintenance and cell fate  
31 decision in downstream progenitors. In this work we describe different roles that Notch plays in  
32 the lymph gland. We show that Notch, activated by its ligand Serrate, expressed at the  
33 Posterior Signaling Center, is required for Core Progenitor maintenance. We define a novel  
34 population of blood cell progenitors that we name Distal Progenitors, where Notch, activated  
35 by Serrate expressed in cells at the Medullary Zone/Cortical Zone boundary, regulates a binary  
36 decision between Plasmacyte and Crystal Cell fates. Thus, Notch plays context-specific  
37 functions in different blood cell progenitor populations of the *Drosophila* lymph gland.

38

39

40

41

42

43

44

45

46

47

48

49

50

51

52

53

54

## 55 Introduction

56 Hematopoiesis in *Drosophila* larvae takes place predominantly at the Lymph Gland (LG), which  
57 is composed of two primary lobes symmetrically localized at both sides of the dorsal vessel, and  
58 smaller posterior lobes that follow a similar array (1) (**Fig. 1a**). At the primary lobes, blood  
59 progenitors (prohemocytes) differentiate into myeloid-like lineages through evolutionary  
60 conserved mechanisms, making the LG an attractive model to explore the pathways involved in  
61 normal and oncogenic hematopoiesis (2-4). At the 3<sup>rd</sup> larval instar, prohemocytes are compactly  
62 arranged in an internal region of the primary lobe, called Medullary Zone (MZ), characterized by  
63 the expression of the JAK/STAT receptor *domeless* (*dome*) (**Fig. 1a, b**) (1, 5, 6). Maturing  
64 hemocytes are found in the peripheric region of the lobe, called Cortical Zone (CZ), which can  
65 be identified by the expression of the Von Willebrand-like factor *hemolectin* (*hml*) (**Fig. 1a, b**)  
66 (1). An Intermediate Progenitor (IP) population has been described at the MZ/CZ boundary,  
67 defined by the expression of both *dome* and *hml* (**Fig. 1b**), but its physiological relevance  
68 remains poorly defined (2, 7). Two types of differentiated populations of hemocytes occur at  
69 the CZ: Plasmatocytes (PLs) and Crystal Cells (CCs) (**Fig. 1a**), whereas a third cell type, the  
70 Lamellocytes, differentiate only following specific immune challenges. PLs, which constitute the  
71 bulk (95%) of mature hemocytes, are macrophages that retain *hml* expression, while they also  
72 express the receptors Nimrod (or P1-antigen) and Eater, both of them important for recognition  
73 of bacteria (8-10). The CCs, named after their cytoplasmic inclusions of Prophenoloxdase  
74 (ProPO), mediate melanization of pathogens and wounds, and constitute 5% of the total  
75 number of mature hemocytes. Mature CCs are thus characterized by the expression of ProPO,  
76 and no longer express the *hml* marker, characteristic of other CZ cells (5, 11). A population of  
77 CC Progenitors can also be identified at the CZ by the expression of the RUNX transcription  
78 factor Lozenge (Lz), homolog of the human AML1/Runx1 protein, frequently altered in Acute  
79 Myeloid Leukemias (1, 12). Another remarkable LG region, termed Posterior Signaling Center  
80 (PSC), occurs at the posterior tip of each primary lobe (**Fig. 1b**). It has been reported to function  
81 as the niche that maintains the progenitor population of the MZ in an undifferentiated state  
82 (13-15). PSC cells express the homeobox protein Antennapedia (Antp) (14), the signaling  
83 molecule Hedgehog (Hh) (14), the Notch ligand Serrate (Ser) (16), and the gene *collier* (*col*),  
84 ortholog of the mammalian Early B-cell Factor (EBF) (6, 17). Hh expressed at the PSC targets the  
85 Medullary Zone and is required to restrain progenitor differentiation (14). Recently the notion  
86 that the PSC functions as a hematopoietic niche has been challenged, as genetic ablation of this  
87 structure did not alter progenitor maintenance nor steady-state blood cell differentiation (18,  
88 19).

89 Notch is a conserved signaling pathway utilized repeatedly during development of all metazoa.  
90 It is typically involved in cell differentiation, binary cell fate decisions, cell proliferation and cell  
91 survival (20). The Notch receptor, which gives the name to the pathway, can be activated by its  
92 transmembrane ligands Serrate (Ser) or Delta (DI) expressed in adjacent cells (**Fig. 1c**). Once this  
93 interaction takes place, Notch undergoes two consecutive cleavage events, resulting in the

94 release of the Notch Intracellular Domain (NICD), which migrates into the nucleus and binds the  
95 transcription factor Suppressor of Hairless (Su(H)). The complex formed by NICD and Su(H)  
96 recruits transcriptional co-activators, thereby inducing transcription of Notch target genes. This  
97 canonical Notch pathway was reported to operate in *hml*-positive cells of the Cortical Zone to  
98 specify the CC fate (16, 21, 22). The source of Notch ligand in this context is Serrate expressed  
99 at cells localized at the MZ/CZ boundary (16, 23). Non-canonical ligand-independent Notch  
100 signaling is afterwards required for CC maturation and survival (22).

101 In mammalian hematopoiesis, Notch pathway functions have been explored quite extensively,  
102 although with contrasting results. Notch receptors (Notch 1-4) are expressed in Hematopoietic  
103 Stem Cells, hematopoietic progenitors and mature blood cells, suggesting that Notch is  
104 required at multiple stages of the differentiation cascade (24). Notch functions in mammalian  
105 hematopoietic stem cells are controversial (25). Results in mouse models suggest that it is  
106 dispensable for their maintenance (26, 27), however *in vitro* conflicting evidences favoring  
107 either a function of Notch in HSC differentiation (28, 29), or a requirement for HSC maintenance  
108 have been reported (30-32). It is however well established that in lymphoid progenitors Notch  
109 promotes differentiation and proliferation of T lymphocytes at the expense of B lymphocytes  
110 (33, 34). Given the involvement of Notch in mammalian hematopoiesis, it is not surprising that  
111 alterations of this pathway are associated with several types of leukemia (35).

112 Because of the diverse, yet unclear functions of Notch in mammalian hematopoiesis, and given  
113 the conservation that occurs between the mechanisms controlling fly and mammalian blood  
114 cell development, we sought to explore the functions that the Notch pathway plays in  
115 *Drosophila* blood cell progenitors. We show here that Notch has distinct functions in two  
116 different populations of hemocyte progenitors: 1) In the recently described “Core progenitors”  
117 (36) Notch is required for maintenance of an undifferentiated state, a function that depends on  
118 Ser expressed at the PSC; and 2) In Distal Progenitors, a cell population defined in this paper,  
119 Notch controls a binary decision towards a PL or a CC fate. This binary Notch-dependent choice  
120 depends on Ser expressed in cells at the MZ/CZ boundary. Thus, Notch plays context-specific  
121 functions in two different cell progenitor populations during *Drosophila* hematopoiesis.

122

## 123 **Results**

### 124 ***Redefining progenitor cell populations of the Medullary Zone***

125 Before analyzing Notch functions in *Drosophila* blood cell progenitors, we sought to define  
126 precisely the different populations of progenitors that occur at the MZ. Cells of the MZ of  
127 wandering 3<sup>rd</sup> instar larvae lymph glands express *domeMESO* and include a subpopulation of  
128 internal cells, the Core Progenitors, characterized by the expression of *tepIV* (36). It is unclear in  
129 the literature whether all *domeMESO*-expressing cells that are negative for *tepIV* coexpress  
130 *hml*, and can be considered Intermediate Progenitors. We found that this is not the case: In

131 larvae that coexpress the Blue Fluorescent Protein (BFP) under a *tepIV*-Gal4 driver (*tepIV* >  
132 BFP), and GFP directly driven by a *domeMESO* promoter (*domeMESO*-GFP), along with dsRed  
133 controlled directly by an *hml* promoter (*hml*-dsRed), three distinct cell populations can be  
134 recognized: 1) Core Progenitors positive for both *tepIV* > BFP and *domeMESO*-GFP (**Fig. 1d**,  
135 region 1); 2) Cells positive only for *domeMESO*-GFP (**Fig. 1d**, region 2); and 3) Intermediate  
136 Progenitors in which *domeMESO*-GFP and *hml*-dsRed signals overlap (**Fig. 1d**, region 3). Thus,  
137 an uncharacterized population of *domeMESO* progenitors which do not express *tepIV* or *hml*  
138 occurs in the lymph gland. We henceforth propose the name “Distal Progenitors” for this  
139 particular population, in reference to their distal location from the dorsal vessel and Core  
140 Progenitors. Interestingly, the membrane receptor Eater, often considered a PL-specific marker  
141 (10, 37), is also expressed in Distal Progenitors of wandering 3<sup>rd</sup> instar larvae (**Fig. 1e**, region 2),  
142 whereas it is barely detectable in Core Progenitors (**Fig. 1e**, region 1).

143 We conclude that three distinct populations of hemocyte progenitors occur at the Medullary  
144 Zone of 3<sup>rd</sup> instar larvae lymph glands: 1) Core Progenitors, which co-express *tepIV* and  
145 *domeMESO*; 2) Distal Progenitors that are positive for *domeMESO* but negative for *tepIV* and  
146 *hml*; and 3) Intermediate Progenitors, which co-express *domeMESO* and *hml* (**Fig. 1f**).

147

#### 148 ***The Notch pathway is required for Core Progenitor maintenance***

149 Notch expression is widespread throughout the lymph gland, suggesting that this pathway  
150 might operate in various cell types (**Fig. 2a**, upper). We initially analyzed Notch function in Core  
151 Progenitors by expressing a *notch* RNAi with *tepIV*-Gal4 (**Fig 2a**, middle), and observed a clear  
152 reduction of Core Progenitors (**Fig. 2a, b**), while both Plasmacytes (PLs) and Crystal Cells  
153 (CCs), increased significantly (**Fig. 2b**). The number of cells of the PSC remained unaltered (**Fig.**  
154 **S1a**). As mentioned above, in wandering 3<sup>rd</sup> instar larvae the receptor Eater is expressed in  
155 Distal Progenitors, while it is almost undetectable in Core Progenitors, so we utilized Eater as  
156 another marker to assess the effect of Notch on progenitor populations. Notch silencing with  
157 *tepIV*-Gal4 resulted in a clear expansion of the *eater* expression domain (**Fig. 2c**), confirming  
158 that Notch is necessary for Core Progenitor maintenance. Consistent with this, silencing of  
159 another component of the canonical Notch pathway, the transcription factor Suppressor of  
160 Hairless (Su(H)), also provoked a reduction of Core Progenitors, while PLs and CCs increased  
161 significantly (**Fig. 2d**). Altogether, these results suggest that the Notch pathway is required cell-  
162 autonomously for maintenance of Core Progenitors in an undifferentiated state.

163 We next analyzed whether over-activation of the Notch pathway provokes the opposite  
164 phenotype, namely an increase of Core Progenitors and general differentiation impairment.  
165 This was not the case, as over-expression with *tepIV*-Gal4 of a full-length Notch construct (**Fig.**  
166 **S1b**) or Su(H) did not alter Core Progenitor, PL or CC populations (**Fig. S1c, d**). These results  
167 suggest that endogenous activity of the Notch pathway is already sufficient to prevent  
168 excessive differentiation of Core Progenitors. It was recently reported that Notch is expressed

169 transiently at the 1<sup>st</sup> larval instar (L1) in a small group of Hematopoietic Stem Cells (HSCs) (38),  
170 so we analyzed the possibility that the phenotype that we observed in Core Progenitors stems  
171 from an alteration of Notch function in L1 HSCs. To investigate this, we used a thermosensitive  
172 Gal80 construct to silence Notch expression only from mid-second larval instar onwards (**Fig.**  
173 **S1e**, upper). The results were identical to those in which Notch was constitutively silenced (**Fig.**  
174 **S1e** and **Fig. 2b**), ruling out the possibility that the loss of Core Progenitors observed after  
175 Notch silencing depends on an early role in L1 HSCs.

176 The findings shown in this section are consistent with a requirement of the Notch pathway for  
177 maintenance of Core Progenitors in an undifferentiated state.

178

### 179 ***Serrate expressed at the Posterior Signaling Center is required for Core progenitor*** 180 ***Maintenance***

181 As a next step, we studied the identity and source of the ligand for Notch activation in Core  
182 Progenitors. *Serrate* (*ser*) is expressed at high levels in PSC cells (1, 14, 16, 23), although no  
183 functions have been yet attributed to this expression. Since the PSC and Core Progenitors are in  
184 close proximity, and filopodia that emanate from PSC cells may play a role in transmitting  
185 signals to MZ progenitors (14), we asked whether Ser expressed at the PSC activates Notch for  
186 Core Progenitor maintenance. First, we silenced Ser at the PSC with an *antp*-Gal4 driver, and  
187 observed an increased number of PLs and CCs (**Fig. 3a**), indicating that Ser is required at the PSC  
188 to limit differentiation. In line with this, analysis of *eater*-dsRed expression following *antp*-Gal4  
189 dependent silencing of Ser revealed a clear reduction of Core Progenitors (*eater*-negative) (**Fig.**  
190 **3b**). These results indicate that Ser is required specifically at the PSC for Core Progenitors  
191 maintenance.

192 Recently, the notion that the PSC functions as a hematopoietic niche has been challenged, as  
193 *antp*-Gal4 driven Reaper expression (i.e. apoptotic ablation of the PSC) did not alter PL or CC  
194 differentiation (18). In that study, genetic ablation of the PSC was confirmed at L3 stage by the  
195 lack of expression of two classical PSC markers, Hh and Antp, whereas Ser expression was not  
196 assessed (18). We thus analyzed if *ser* expressing cells are still present in LGs in which the PSC  
197 was genetically ablated. Ablation was induced from L2 stage onwards by using a Gal80  
198 thermosensitive construct to prevent Reaper expression and lethality at earlier stages. We  
199 monitored the expression of a *ser*-*LacZ* construct (1, 14, 16, 23, 39), and consistently observed  
200 the presence of *ser*-expressing cells in LGs where *antp*-positive cells were ablated (**Fig 3c**,  
201 lower). Importantly, in wild-type lymph glands we observed PSC cells that express *ser* but not  
202 *antp* (**Fig. 3c**, upper), suggesting that the PSC might encompass a mixed population of cells, with  
203 a large proportion of them co-expressing *antp* and *ser*, while some cells express *ser* but not  
204 *antp*. These observations are consistent with a model in which, after genetic ablation of the  
205 *antp*<sup>+</sup> cells of the PSC, the remaining *ser*<sup>+</sup>, *antp*<sup>-</sup> PSC cells are sufficient to sustain normal Core  
206 Progenitor maintenance and hemocyte differentiation. Noteworthy, after *antp*-driven ablation,

207 a negative correlation between surviving *ser*<sup>+</sup>, *antp*<sup>-</sup> PSC cells and hemocyte differentiation  
208 occurs: Lymph glands with a small *ser*-positive area at the PSC display greater PLs  
209 differentiation than those with a larger *ser*-positive area at the PSC (**Fig. 3d**). These results  
210 suggest that *ser* expressing cells of the PSC are important for Core Progenitor maintenance, and  
211 that the *ser* expressing cells that survive to *antp*-driven apoptotic cell ablation can support  
212 normal blood cell differentiation.

213

### 214 ***In Distal Progenitors the Notch pathway controls a binary cell fate decision***

215 We have shown above that *notch* silencing with *teplV*-Gal4 provokes enhanced differentiation  
216 of both PLs and CCs (**Fig. 2b**). In sharp contrast, *notch* silencing with *domeMESO*-Gal4 brought  
217 about almost complete loss of CCs accompanied by an increased proportion of PLs (**Figs. 4a and**  
218 **S2a**). Similar results were obtained when *su(H)* was silenced with the same driver (**Fig. 4b**),  
219 suggesting that the Notch pathway promotes CC differentiation in Distal Progenitors, while the  
220 PL fate is inhibited. To further explore this possibility, we over-expressed with *domeMESO*-Gal4  
221 a full-length Notch construct (**Fig. S2b**) or the Notch Intracellular Domain (NICD), and observed  
222 in both cases that PL differentiation was virtually blocked, and CCs increased dramatically (**Fig.**  
223 **4c**). Over-expression of Su(H) with *domeMESO*-Gal4 provoked the same effect (**Fig. 4d**). We  
224 thus conclude that an increase of Notch pathway activity in Distal Progenitors induces CC  
225 differentiation and inhibits PL differentiation.

226 To confirm that the activity of Notch is indeed required for normal differentiation in Distal  
227 Progenitors that are positive for *domeMESO* and negative for *hml* (**Fig. 1d, f**), *notch* silencing  
228 with *domeMESO*-Gal4 was repeated in a genetic background in which *notch* RNAi expression in  
229 cells that co-express *hml* was inhibited by QUAS-Gal80 (*domeMESO*-Gal4 > UAS-*N<sup>RNAi</sup>*; *hml*-QF >  
230 QUAS-Gal80). Silencing of Notch in this genetic background provoked identical effects to those  
231 observed without expression of Gal80 in *hml*-positive cells (**Fig. S2c**). In a control experiment,  
232 *hml*-QF driven expression of QUAS-Gal80 effectively repressed Gal4 activity in the CZ (**Fig. S2d**).  
233 These results confirm that Notch operates in the Distal Progenitors, which express *domeMESO*  
234 but not *hml*.

235 Together, this set of experiments indicates that in Distal Progenitors the Notch pathway  
236 regulates a binary fate decision, promoting CC differentiation while inhibiting the PL fate.

237

### 238 ***Eater is an early Plasmatocyte fate marker in Distal Progenitors***

239 Next, we explored further aspects of this Notch-dependent binary fate decision that takes place  
240 in Distal Progenitors. Noteworthy, a closer look to *eater*-dsRed reporter expression shown in  
241 **Fig. 1e** revealed that *eater*-dsRed can be detected in most Distal Progenitors but is virtually  
242 absent in a few cells within this region (**Fig. 5a**). A possible explanation is that *eater*-expressing  
243 Distal Progenitors at the 3<sup>rd</sup> instar might be already committed towards a PL fate, while those



244 Distal Progenitors with very low *eater* levels are likely committed to become CCs. Consistent  
245 with this notion, we observed at the CZ that *eater*-dsRed expression occurs in most *hml*-positive  
246 cells, while it is excluded from those cells that express the CC progenitor marker Lz (**Fig. 5b**).  
247 Lineage tracing experiments with an *eater*-Gal4 driver revealed that the lineage does not  
248 include CCs (**Fig. 5c**), supporting that *eater* expression in Distal Progenitors marks a Distal  
249 Progenitor subpopulation committed for a PL cell fate. *Eater*-Gal4 driven *notch* silencing or  
250 Notch over-expression did not recapitulate the effects observed when *domeMESO*-Gal4 was  
251 utilized to perform the same manipulations (compare **Figs. 4a, c** with **Fig. S3a**), suggesting that  
252 Notch operates in Distal Progenitors that have not yet begun to express *eater*. The above  
253 observations are consistent with a model in which, at an earlier developmental stage, *eater*-  
254 negative uncommitted Distal Progenitors make the binary cell fate decision regulated by Notch,  
255 while later, *eater* is expressed in cells committed to a PL fate.

256 If *eater* is indeed an early marker for Distal Progenitors committed to a PL fate, its expression  
257 should be controlled by the Notch pathway. We assessed this possibility by over-expressing  
258 Notch with *domeMESO*-Gal4, a treatment that induces massive differentiation to CCs (**Fig. 4c**),  
259 and observed almost complete absence of *dome*<sup>+</sup>, *eater*<sup>+</sup> double-positive Distal Progenitors (**Fig.**  
260 **5d**). Conversely, Notch silencing provoked a complete conversion of *dome*<sup>+</sup> *eater*<sup>-</sup> progenitors  
261 into *dome*<sup>+</sup>, *eater*<sup>+</sup> double-positive Distal Progenitors (**Fig. 5d**). These observations suggest that  
262 *eater* expressed in Distal Progenitors is an early marker for a Notch-dependent binary fate  
263 decision, labeling cells committed to a PL fate.

264

### 265 ***Serrate expressed at the MZ/CZ boundary regulates the cell fate decision in Distal Progenitors***

266 Groups of Serrate-expressing cells lying next to the MZ/CZ boundary, which instruct progenitors  
267 to acquire a CC fate have been previously reported (16, 23). We therefore investigated whether  
268 these cells provide the ligand for the Notch-dependent binary cell fate decision in Distal  
269 Progenitors. We noticed that a major proportion of these Ser-expressing cells, but not the Ser-  
270 expressing cells of the PSC, co-express *domeMESO* (**Fig. 6a**), so we utilized *domeMESO*-Gal4 to  
271 manipulate Ser expression. Silencing of *ser* with *domeMESO*-Gal4 virtually blocked CC  
272 differentiation, while it increased PL proportion (**Fig. 6b**), mimicking the effect of *notch* silencing  
273 with the same Gal4 driver (**Fig. 4a**). In agreement, overexpression of Ser rendered the opposite  
274 results, increasing CCs and reducing PLs (**Fig. 6c**). Thus Ser expressed in cells of the MZ/CZ  
275 boundary is required for Notch activation in Distal Progenitors, controlling the binary cell fate  
276 choice. The E3 ubiquitin ligase *neutralized* (*neu*) is necessary for Ser endocytosis and Notch  
277 activation in neighboring cells (40). Mimicking the results obtained after *ser* silencing with  
278 *domeMESO*-Gal4, expression of a *neu* RNAi with the same driver reduced CC number and  
279 increased PLs (**Fig. 6d**), further supporting the notion that Ser expressed at the MZ/CZ boundary  
280 activates Notch signaling for the binary cell fate decision in Distal Progenitors.

281

## 282 Discussion

283 In mammals, Notch receptors (Notch 1-4) are expressed in HSCs, hematopoietic progenitors  
284 and mature blood cells, suggesting that Notch is required at multiple levels of blood cell  
285 differentiation. Particularly, the role of the Notch pathway in HSC maintenance has been  
286 explored in depth, although with contrasting results. Some experiments in cell culture suggest  
287 that Notch is required for HSC maintenance (30-32), while others suggest that it promotes HSC  
288 differentiation towards the myeloid lineage (28, 29). Works *in vivo* in which interactions with  
289 the hematopoietic niche is still present, and therefore recapitulate better a physiologic  
290 situation, also yielded conflicting results. Studies utilizing conditional knock-out mice affecting  
291 different elements of the canonical Notch pathway suggested that Notch is dispensable for HSC  
292 maintenance (26, 27), while others indicated that alterations of Notch signaling are associated  
293 with development of myeloproliferative disease (MPD), characterized by accumulation of  
294 mature cells of the myeloid lineage (41). Thus, the role of Notch in adult HSC homeostasis is at  
295 least controversial and requires further examination. Many aspects of mammalian and  
296 *Drosophila* hematopoiesis are conserved, particularly at the level of the transcription factors  
297 and signaling pathways involved (2-4). One striking parallelism between *Drosophila* and  
298 mammalian models is the expression in the hematopoietic niche of the Notch ligand Serrate  
299 (Ser)/Jagged (JAG). While Ser is expressed in cells of the *Drosophila* PSC (16), mammalian JAG1  
300 and JAG2 expression has been detected in different bone marrow cell types that fulfill niche  
301 functions, including endothelial cells and cells of the hematopoietic stroma (42-44). The wide  
302 array of genetic tools available in *Drosophila* allow for manipulations of gene expression with an  
303 exquisite temporal and spatial specificity that is currently not possible to the same extent in  
304 mammalian systems. Thus, the utilization of the fly model may provide clues for addressing  
305 unresolved issues related to Notch functions in mammalian hematopoiesis.

306 In the current work, we have analyzed biological properties of *Drosophila* blood cell  
307 progenitors. This analysis led us to redefine the progenitor subpopulations of the larval lymph  
308 gland. A novel progenitor population, the “Distal Progenitors” that are positive for *domeMESO*  
309 and negative for both *teplV* and *hml*, occurs at the medullary zone. Our results strongly suggest  
310 that the binary fate decision between PLs and CCs is made in naïve Distal Progenitors at early  
311 larval stages, while later in development, at wandering 3<sup>rd</sup> instar larvae, the PL-specific marker  
312 *eater* is expressed in most but not all Distal Progenitors, marking the cells that are already  
313 committed to a PL fate. The remaining Distal Progenitors with low *eater* levels are committed to  
314 become CCs, as suggested by *eater* lineage tracing, as well as by *eater* and Lz mutually exclusive  
315 expression in *hml*-positive cells. Thus, the Medullary Zone, in wandering 3<sup>rd</sup> instar larvae,  
316 encompasses an undifferentiated population of cells, the Core Progenitors, and a second  
317 population, the Distal Progenitors, which have already been instructed to become either PLs or  
318 CCs.

319 We have found that Notch, which is expressed throughout the lymph gland, plays distinct  
320 functions in Core Progenitors or Distal Progenitors (**Fig. 7**). In Core Progenitors Notch is required

321 for maintenance of the undifferentiated state; our results thus contribute to the incipient  
322 characterization of the Core Progenitor subpopulation, in which *collier (col)* is expressed at low  
323 but physiologically relevant levels (36). We found that Notch function in Core Progenitors  
324 depends on Ser that is expressed at the PSC. This Ser expression has been reported before (1,  
325 14, 16, 23), but its function remained elusive. Filopodia emanating from PSC cells and  
326 intermingling between cells of the MZ have been described, and were proposed to participate  
327 in Hedgehog signaling (14). Given our observation that Ser expressed at the PSC is necessary for  
328 Notch activation in Core Progenitors, and considering that direct cell-cell interactions are  
329 required for Notch stimulation by its ligands, it seems reasonable to hypothesize that the  
330 filopodia that emanate from the PSC may play a role in Notch signaling as well (6).

331 It has been shown that genetic ablation of the PSC by expression of the proapoptotic protein  
332 Reaper (Rpr) does not alter Core Progenitor maintenance nor steady-state differentiation,  
333 challenging the notion that the PSC functions as a hematopoietic niche (18). Using the same  
334 PSC-ablation protocol with *antp*-Gal4 driven expression of Rpr from L2 stage onwards, we  
335 detected the presence of *ser*-positive cells in the PSC that escaped genetic ablation. Moreover,  
336 in wild-type lymph glands the PSC includes a subpopulation of cells that are *ser*-positive and  
337 *antp*-negative (*ser*<sup>+</sup>, *antp*<sup>-</sup>). It is therefore likely that those *ser*-positive cells that survived *antp*-  
338 Gal4 induced genetic ablation are responsible for maintaining Core Progenitors and for  
339 sustaining normal progenitor differentiation.

340 We have found that in Distal Progenitors Notch fulfills a totally different function; it regulates a  
341 binary cell fate decision, promoting CC differentiation, and inhibiting differentiation of PLs (**Fig.**  
342 **7**). We propose that the activation of the Notch pathway in Distal Progenitors is achieved  
343 through direct interaction of early naive Distal Progenitors with Ser-expressing cells localized at  
344 the MZ/CZ boundary, thereby inducing CC differentiation and repressing the PL fate. On the  
345 other hand, naive Distal Progenitors that do not contact these Ser-expressing cells undergo a  
346 default differentiation program towards a PL fate (**Fig. 7**). Our finding that Notch regulates in  
347 Distal Progenitors a binary cell fate decision between a PL and a CC fate is in line with previous  
348 results by Tokusumi et al. (45): These authors utilized the allelic combination *su(H)*<sup>1</sup>/*su(H)*<sup>115B</sup>,  
349 and observed a total block of CC differentiation accompanied by massive differentiation of PLs  
350 that invaded the MZ. According to the model proposed in the current study (**Fig. 7**), this is  
351 indeed the expected outcome of Tokusumi et al. experiments (45), where a combined effect of  
352 Core Progenitor loss, along with inhibition of the CC fate and default differentiation towards the  
353 PL fate in Distal Progenitors is expected. It is still an open issue whether early fate specification  
354 in Distal Progenitors establishes the final (95:5) proportion of PLs versus CCs observed at the  
355 Cortical Zone, or if alternatively, the fate specification in Distal Progenitors brings about an  
356 initial 50:50 proportion of cells committed to one versus the other fate, followed by increased  
357 proliferative capacity of PL-committed Distal Progenitors.

358 The Notch pathway has been previously demonstrated to be necessary and sufficient for CC  
359 specification at the CZ (16, 21, 22). Our results suggest that Notch-dependent CC specification

360 occurs earlier in Distal Progenitors, and that Notch is probably required at later stages to  
361 sustain the original specification. Two works support this notion: Firstly, Krzemien et al. (46)  
362 utilized a clone labelling strategy at different larval stages, reaching the conclusion that blood  
363 cell progenitors of early L2 larvae, which have not yet developed a CZ, have already restrained  
364 their differentiating potential, either towards a PL or a CC fate. Secondly, at later stages of CC  
365 development, namely when Lz expression begins in unipotent CC progenitors at the CZ, it has  
366 been reported that Notch inhibits the expression of PL-specific genes (47). In this study, gene  
367 expression manipulations performed with *Iz-Gal4* demonstrated that the Notch target gene  
368 *klumpfuss (klu)* mediates repression of P1 expression in CC progenitors, thereby stabilizing CC  
369 commitment (47). We induced *klu* silencing with *domeMESO-Gal4* in multipotent Distal  
370 Progenitors, and did not observe alterations of PL or CC differentiation (data not shown). This  
371 observation suggests that Notch target genes that regulate the early fate decision in Distal  
372 Progenitors, and those target genes that mediate CC-fate stabilization later at the CZ may be  
373 different. The identity of the Notch target genes that regulate initial cell fate determination in  
374 Distal Progenitors are not known and should be addressed in future investigations.

375 Notch function as a regulator of the cell fate choice in Distal Progenitors is remarkably similar to  
376 the role of Notch reported in the control of a binary cell fate decision in mammalian lymphoid  
377 progenitors (24, 33, 34, 48, 49). In this case, inhibition of the Notch pathway induces a default  
378 differentiation program towards a B lymphocyte fate, while the T lymphocyte fate is abolished  
379 (33, 34, 48). Conversely, over-activation of the Notch pathway induces a T cell fate, while B cell  
380 differentiation is inhibited (49). Even though *Drosophila* progenitors are considered myeloid-  
381 like lineage cells, this similarity in Notch-dependent blood progenitor cell fate decision with the  
382 mammalian lymphoid lineage suggests a primitive mechanism of cell communication that  
383 determines a balance of blood cell types in hematopoiesis.

384 The Notch pathway is therefore employed several times during hematopoiesis at the lymph  
385 gland. First: A possible role in HSC at the 1<sup>st</sup> larval instar (38); second: It is required for  
386 maintenance of Core Progenitors (this study); third: In Distal Progenitors it regulates the binary  
387 cell fate choice between PLs and CCs (this study); fourth: At the CZ, it is involved in fate  
388 stabilization in CC progenitors (47), and later it is required for CC maturation and survival (22).  
389 With the development of increasingly sophisticated genetic tools in mammalian systems, future  
390 studies may determine if Notch fulfills comparable context-specific functions throughout the  
391 mammalian hematopoietic hierarchy.

392

## 393 **Materials and Methods**

### 394 *Fly Strains and crosses*

395 The following *Drosophila* strains were used: *domeMESO-GFP*; *hml-dsRed*; *domeMESO-Gal4*;  
396 *antp-Gal4* (U. Banerjee), *ser-LacZ* (A. Bachmann); *eater-dsRed*; *eater-Gal4* (RA. Schulz). The

397 following stocks were obtained from the Bloomington Stock Center: UAS-GFP; UAS-BFP; *GFP*  
398 RNAi; QUAS-GFP; QUAS-Gal80; *hml-Gal4*; *hml-QF*; *notch* RNAi; *notch* RNAi (2); *su(H)* RNAi; *tub*-  
399 Gal80<sup>ts</sup>; UAS-Su(H); UAS-Notch; UAS-NICD; *ser* RNAi; UAS-Ser; *neu* RNAi; UAS-RedStinger, UAS-  
400 Flp, Ubi-p63E(FRT.STOP)Stinger (G-TRACE, (50)). *TepIV-Gal4* was obtained from the Vienna  
401 *Drosophila* Resource Center. All experimental crosses were performed at 25 °C and F1 larvae  
402 were incubated at 29 °C to maximize Gal4 activity, with the exception of experiments involving  
403 *tub-Gal80<sup>ts</sup>*, in which larvae were kept at 18 °C and then transferred to 29 °C to induce Gal4  
404 activity. Experiments involving *notch* RNAi (2) and *su(H)* RNAi were performed in a genetic  
405 background that included UAS-Dicer2 to enhance silencing.

#### 406 *Immunohistochemistry*

407 Lymph glands were processed and stained as previously described (5): lymph glands were  
408 dissected from third-instar larvae (unless otherwise stated) in 1× PBS, fixed in 4%  
409 formaldehyde/1× PBS for 30 min, washed three times in 1×PBS with 0.4% Triton-X (1× PBST) for  
410 15 min each, blocked in 10% normal goat serum/1× PBST for 30 min, followed by incubation  
411 with primary antibodies overnight at 4°C in blocking solution. Primary antibodies were washed  
412 three times in 1× PBST for 15 min each, re-blocked for 30 min, followed by incubation with  
413 secondary antibodies for 2 hr at room temperature. Samples were then washed three times in  
414 1× PBST prior to mounting on glass slides in glycerol with Mowiol 4-88 anti-fade agent (EMD  
415 Millipore Corp., Billerica, MA). The following primary antibodies were used: rabbit α-βgal  
416 (Cappel), rabbit α-GFP (ThermoFisher, Waltham, MA), mouse α-Lz, mouse α-βgal, mouse α-  
417 Notch, mouse α-Antp (Developmental Studies Hybridoma Bank, Iowa City, IA), mouse α-P1 (gift  
418 from I. Ando), rabbit α-ProPO (gift from G. Christophides). Alexa Fluor 488-, Alexa Fluor 647-,  
419 DyLight 405- and Cy3- conjugated secondary antibodies were used (Jackson ImmunoResearch,  
420 West Grove, PA).

#### 421 *Image acquisition and processing*

422 Lymph glands were registered in a Zeiss LSM 510 confocal microscope, either as Z-stacks or  
423 single confocal planes as indicated in each case. Images were processed using ImageJ software.  
424 Quantification of the area occupied by the indicated markers was performed using whole Z-  
425 projections of confocal stacks or single confocal planes as mentioned in each case, and is  
426 expressed as the area occupied by the marker relative to the total lobe area. In the case of CCs,  
427 the total number of CCs relative to the total lobe area was quantified.

#### 428 *Statistical analysis*

429 Two-tailed unpaired Student's t-tests or one-way ANOVAs (GraphPad Prism software) were  
430 used. The threshold for statistical significance was established as \*p < 0.05, \*\*p < 0.01 or \*\*\*p  
431 < 0.001.

432

## 433 **Acknowledgements**

434 We thank U. Banerjee lab members for sharing knowledge and expertise on lymph gland work.  
435 RA. Schulz, A. Bachman and U. Banerjee for fly stocks; I. Ando and G. Christophides for the kind  
436 gift of mouse  $\alpha$ -P1 and rabbit  $\alpha$ -ProPO antibodies. The mouse  $\alpha$ -Lz (U.Banerjee), mouse  $\alpha$ - $\beta$ gal  
437 (J.R. Sanes), mouse  $\alpha$ -Notch (S. Artavanis-Tsakonas) and mouse  $\alpha$ -Antp (D. Brower) antibodies,  
438 developed by the indicated investigators, were obtained from the Developmental Studies  
439 Hybridoma Bank, created by the NICHD of the NIH and maintained at The University of Iowa,  
440 Department of Biology, Iowa City, IA 52242. Stocks obtained from the Bloomington Drosophila  
441 Stock Center (NIH P40OD018537) and the Kyoto Stock Center were used in this study. We  
442 thank members of the Wappner lab for discussion and comments on the manuscript.

443

## 444 **Competing interests**

445 The authors declare no competing interests.

446

## 447 **Funding**

448 DBO is a fellow of Agencia Nacional de Promoción Científica y Tecnológica (ANPCyT) and was  
449 travel fellow from The Company of Biologists; MJK is a Career Investigator of Consejo Nacional  
450 de Investigaciones Científicas y Técnicas (CONICET); LD is member of FBMC (Universidad de  
451 Buenos Aires); PW is a Career Investigator of CONICET. This work was supported by ANPCyT  
452 grants PICT 2014-0649 and PICT 2015-0372 to PW.

453

## 454 **References**

- 455 1. Jung SH, Evans CJ, Uemura C, Banerjee U. The Drosophila lymph gland as a developmental  
456 model of hematopoiesis. *Development*. 2005;132(11):2521-33.
- 457 2. Banerjee U, Girard JR, Goins LM, Spratford CM. *Drosophila* as a Genetic Model for  
458 Hematopoiesis. *Genetics*. 2019;211(2):367-417.
- 459 3. Crozatier M, Vincent A. Drosophila: a model for studying genetic and molecular aspects of  
460 haematopoiesis and associated leukaemias. *Dis Model Mech*. 2011;4(4):439-45.
- 461 4. Evans CJ, Sinenko SA, Mandal L, Martinez-Agosto JA, Hartenstein V, Banerjee U. Genetic  
462 Dissection of Hematopoiesis Using Drosophila as a Model System. 2007;18:259-99.
- 463 5. Evans CJ, Liu T, Banerjee U. Drosophila hematopoiesis: Markers and methods for molecular  
464 genetic analysis. *Methods*. 2014;68(1):242-51.
- 465 6. Krzemien J, Dubois L, Makki R, Meister M, Vincent A, Crozatier M. Control of blood cell  
466 homeostasis in Drosophila larvae by the posterior signalling centre. *Nature*. 2007;446(7133):325-8.
- 467 7. Krzemien J, Oyallon J, Crozatier M, Vincent A. Hematopoietic progenitors and hemocyte lineages  
468 in the Drosophila lymph gland. *Developmental biology*. 2010;346(2):310-9.

- 469 8. Kurucz E, Markus R, Zsamboki J, Folkl-Medzihradzky K, Darula Z, Vilmos P, et al. Nimrod, a  
470 putative phagocytosis receptor with EGF repeats in *Drosophila* plasmatocytes. *Curr Biol*. 2007;17(7):649-  
471 54.
- 472 9. Kurucz E, Vaczi B, Markus R, Laurinyecz B, Vilmos P, Zsamboki J, et al. Definition of *Drosophila*  
473 hemocyte subsets by cell-type specific antigens. *Acta Biol Hung*. 2007;58 Suppl:95-111.
- 474 10. Kocks C, Cho JH, Nehme N, Ulvila J, Pearson AM, Meister M, et al. Eater, a transmembrane  
475 protein mediating phagocytosis of bacterial pathogens in *Drosophila*. *Cell*. 2005;123(2):335-46.
- 476 11. Rizki TM, Rizki RM, Grell EH. A mutant affecting the crystal cells in *Drosophila melanogaster*.  
477 *Wilehm Roux Arch Dev Biol*. 1980;188(2):91-9.
- 478 12. Lebestky T. Specification of *Drosophila* Hematopoietic Lineage by Conserved Transcription  
479 Factors. *Science*. 2000;288(5463):146-9.
- 480 13. Pennetier D, Oyallon J, Morin-Poulard I, Dejean S, Vincent A, Crozatier M. Size control of the  
481 *Drosophila* hematopoietic niche by bone morphogenetic protein signaling reveals parallels with  
482 mammals. *Proc Natl Acad Sci U S A*. 2012;109(9):3389-94.
- 483 14. Mandal L, Martinez-Agosto JA, Evans CJ, Hartenstein V, Banerjee U. A Hedgehog- and  
484 Antennapedia-dependent niche maintains *Drosophila* haematopoietic precursors. *Nature*.  
485 2007;446(7133):320-4.
- 486 15. Mondal BC, Mukherjee T, Mandal L, Evans CJ, Sinenko SA, Martinez-Agosto JA, et al. Interaction  
487 between differentiating cell- and niche-derived signals in hematopoietic progenitor maintenance. *Cell*.  
488 2011;147(7):1589-600.
- 489 16. Lebestky T, Jung SH, Banerjee U. A Serrate-expressing signaling center controls *Drosophila*  
490 hematopoiesis. *Genes Dev*. 2003;17(3):348-53.
- 491 17. Crozatier M, Ubeda J-M, Vincent A, Meister M. Cellular Immune Response to Parasitization in  
492 *Drosophila* Requires the EBF Orthologue Collier. *PLOS Biology*. 2004;2(8):e196.
- 493 18. Benmimoun B, Polesello C, Haenlin M, Waltzer L. The EBF transcription factor Collier directly  
494 promotes *Drosophila* blood cell progenitor maintenance independently of the niche. *Proc Natl Acad Sci*  
495 *U S A*. 2015;112(29):9052-7.
- 496 19. Baldeosingh R, Gao H, Wu X, Fossett N. Hedgehog signaling from the Posterior Signaling Center  
497 maintains U-shaped expression and a prohemocyte population in *Drosophila*. *Dev Biol*. 2018;441(1):132-  
498 45.
- 499 20. Bray SJ. Notch signalling in context. *Nat Rev Mol Cell Biol*. 2016;17(11):722-35.
- 500 21. Duvic B, Hoffmann JA, Meister M, Royet J. Notch Signaling Controls Lineage Specification during  
501 *Drosophila* Larval Hematopoiesis. *Current Biology*. 12(22):1923-7.
- 502 22. Mukherjee T, Kim WS, Mandal L, Banerjee U. Interaction between Notch and Hif-alpha in  
503 development and survival of *Drosophila* blood cells. *Science*. 2011;332(6034):1210-3.
- 504 23. Ferguson GB, Martinez-Agosto JA. Yorkie and Scalloped signaling regulates Notch-dependent  
505 lineage specification during *Drosophila* hematopoiesis. *Curr Biol*. 2014;24(22):2665-72.
- 506 24. Liu J, Sato C, Cerletti M, Wagers A. Chapter Twelve - Notch Signaling in the Regulation of Stem  
507 Cell Self-Renewal and Differentiation. In: Kopan R, editor. *Current Topics in Developmental Biology*. 92:  
508 Academic Press; 2010. p. 367-409.
- 509 25. Lampreia FP, Carmelo JG, Anjos-Afonso F. Notch Signaling in the Regulation of Hematopoietic  
510 Stem Cell. *Curr Stem Cell Rep*. 2017;3(3):202-9.
- 511 26. Mancini SJC, Mantei N, Dumortier A, Suter U, MacDonald HR, Radtke F. Jagged1-dependent  
512 Notch signaling is dispensable for hematopoietic stem cell self-renewal and differentiation. *Blood*.  
513 2005;105(6):2340-2.
- 514 27. Maillard I, Koch U, Dumortier A, Shestova O, Xu L, Sai H, et al. Canonical notch signaling is  
515 dispensable for the maintenance of adult hematopoietic stem cells. *Cell stem cell*. 2008;2(4):356-66.

- 516 28. Schroeder T, Just U. Notch signalling via RBP-J promotes myeloid differentiation. *EMBO J.* 2000;19(11):2558-68.
- 517
- 518 29. Schroeder T, Kohlhof H, Rieber N, Just U. Notch signaling induces multilineage myeloid  
519 differentiation and up-regulates PU.1 expression. *J Immunol.* 2003;170(11):5538-48.
- 520 30. Kumano K, Chiba S, Shimizu K, Yamagata T, Hosoya N, Saito T, et al. Notch1 inhibits  
521 differentiation of hematopoietic cells by sustaining GATA-2 expression. *Blood.* 2001;98(12):3283-9.
- 522 31. Vercauteren SM, Sutherland HJ. Constitutively active Notch4 promotes early human  
523 hematopoietic progenitor cell maintenance while inhibiting differentiation and causes lymphoid  
524 abnormalities in vivo. *Blood.* 2004;104(8):2315.
- 525 32. Varnum-Finney B, Xu L, Brashem-Stein C, Nourigat C, Flowers D, Bakkour S, et al. Pluripotent,  
526 cytokine-dependent, hematopoietic stem cells are immortalized by constitutive Notch1 signaling. *Nat*  
527 *Med.* 2000;6(11):1278-81.
- 528 33. Radtke F, Wilson A, Stark G, Bauer M, van Meerwijk J, MacDonald HR, et al. Deficient T cell fate  
529 specification in mice with an induced inactivation of Notch1. *Immunity.* 1999;10(5):547-58.
- 530 34. Han H, Tanigaki K, Yamamoto N, Kuroda K, Yoshimoto M, Nakahata T, et al. Inducible gene  
531 knockout of transcription factor recombination signal binding protein-J reveals its essential role in T  
532 versus B lineage decision. *Int Immunol.* 2002;14(6):637-45.
- 533 35. Kushwah R, Guezguez B, Lee JB, Hopkins CI, Bhatia M. Pleiotropic roles of Notch signaling in  
534 normal, malignant, and developmental hematopoiesis in the human. *EMBO reports.* 2014;15(11):1128-  
535 38.
- 536 36. Oyallon J, Vanzo N, Krzemien J, Morin-Poulard I, Vincent A, Crozatier M. Two Independent  
537 Functions of Collier/Early B Cell Factor in the Control of Drosophila Blood Cell Homeostasis. *PLoS One.*  
538 2016;11(2):e0148978.
- 539 37. Tokusumi T, Shoue DA, Tokusumi Y, Stoller JR, Schulz RA. New hemocyte-specific enhancer-  
540 reporter transgenes for the analysis of hematopoiesis in Drosophila. *Genesis.* 2009;47(11):771-4.
- 541 38. Dey NS, Ramesh P, Chugh M, Mandal S, Mandal L. Dpp dependent Hematopoietic stem cells give  
542 rise to Hh dependent blood progenitors in larval lymph gland of Drosophila. *Elife.* 2016;5.
- 543 39. Bachmann A, Knust E. Dissection of cis-regulatory elements of the Drosophila gene Serrate.  
544 *Development Genes and Evolution.* 1998;208(6):346-51.
- 545 40. Le Borgne R, Remaud S, Hamel S, Schweisguth F. Two Distinct E3 Ubiquitin Ligases Have  
546 Complementary Functions in the Regulation of Delta and Serrate Signaling in Drosophila. *PLOS Biology.*  
547 2005;3(4):e96.
- 548 41. Klinakis A, Lobry C, Abdel-Wahab O, Oh P, Haeno H, Buonamici S, et al. A novel tumour-  
549 suppressor function for the Notch pathway in myeloid leukaemia. *Nature.* 2011;473(7346):230-3.
- 550 42. Varnum-Finney B, Purton LE, Yu M, Brashem-Stein C, Flowers D, Staats S, et al. The Notch  
551 Ligand, Jagged-1, Influences the Development of Primitive Hematopoietic Precursor Cells. *Blood.*  
552 1998;91(11):4084.
- 553 43. Calvi LM, Adams GB, Weibrecht KW, Weber JM, Olson DP, Knight MC, et al. Osteoblastic cells  
554 regulate the haematopoietic stem cell niche. *Nature.* 2003;425(6960):841-6.
- 555 44. Fernandez L, Rodriguez S, Huang H, Chora A, Fernandes J, Mumaw C, et al. Tumor necrosis  
556 factor-alpha and endothelial cells modulate Notch signaling in the bone marrow microenvironment  
557 during inflammation. *Exp Hematol.* 2008;36(5):545-58.
- 558 45. Tokusumi Y, Tokusumi T, Stoller-Conrad J, Schulz RA. Serpent, suppressor of hairless and U-  
559 shaped are crucial regulators of hedgehog niche expression and prohemocyte maintenance during  
560 Drosophila larval hematopoiesis. *Development.* 2010;137(21):3561-8.
- 561 46. Krzemien J, Oyallon J, Crozatier M, Vincent A. Hematopoietic progenitors and hemocyte lineages  
562 in the Drosophila lymph gland. *Dev Biol.* 2010;346(2):310-9.

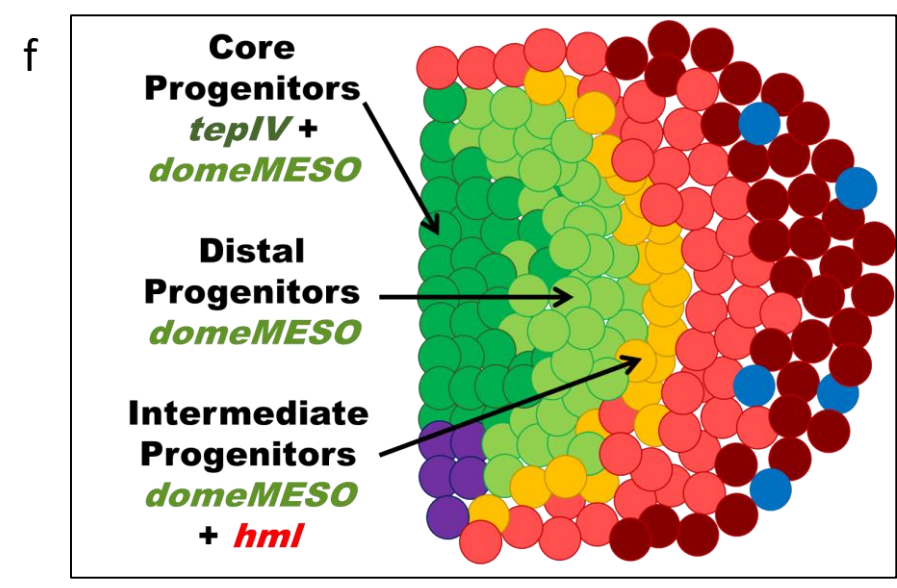
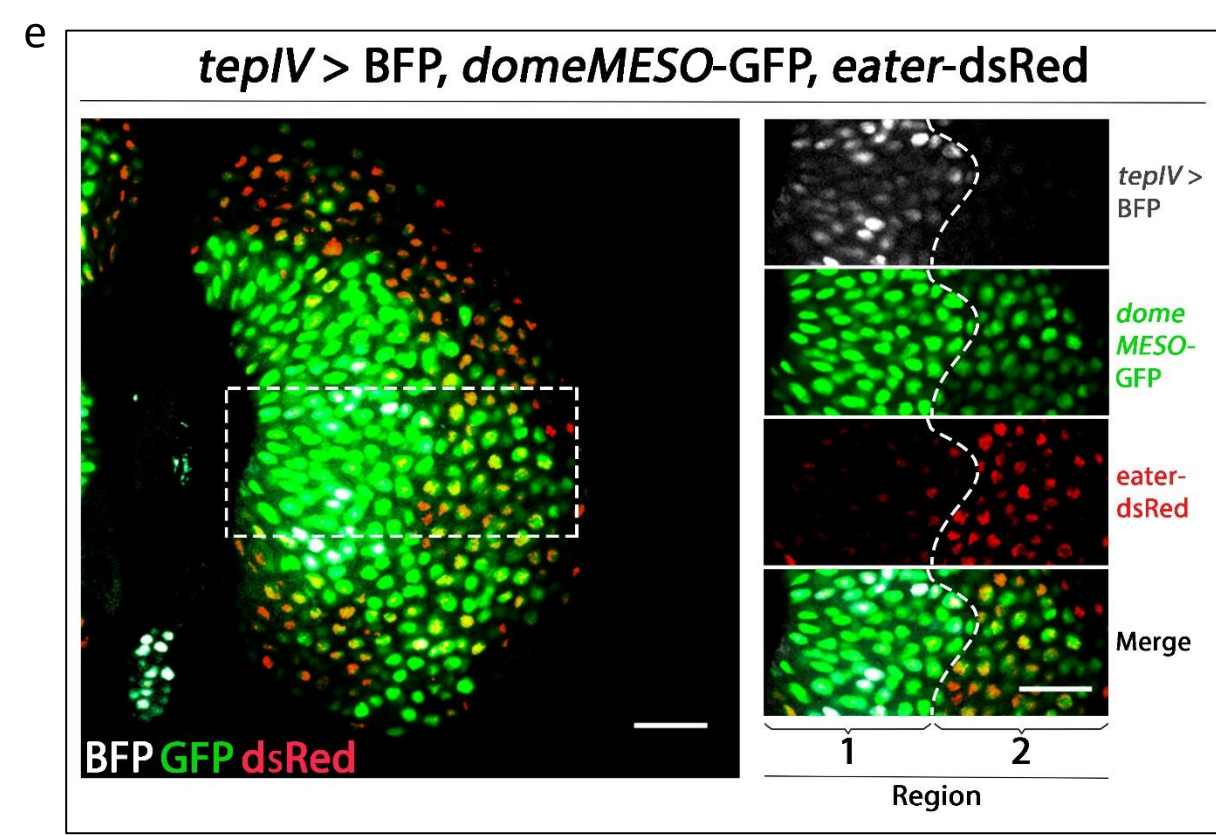
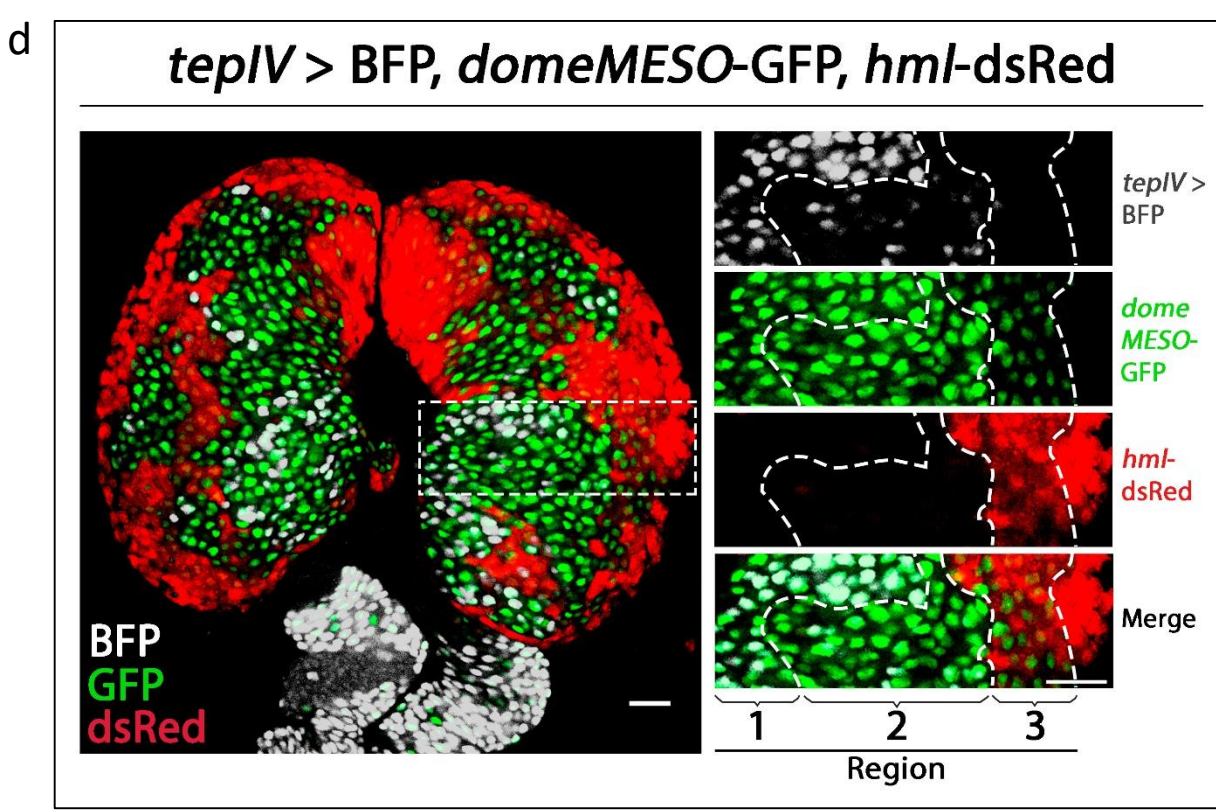
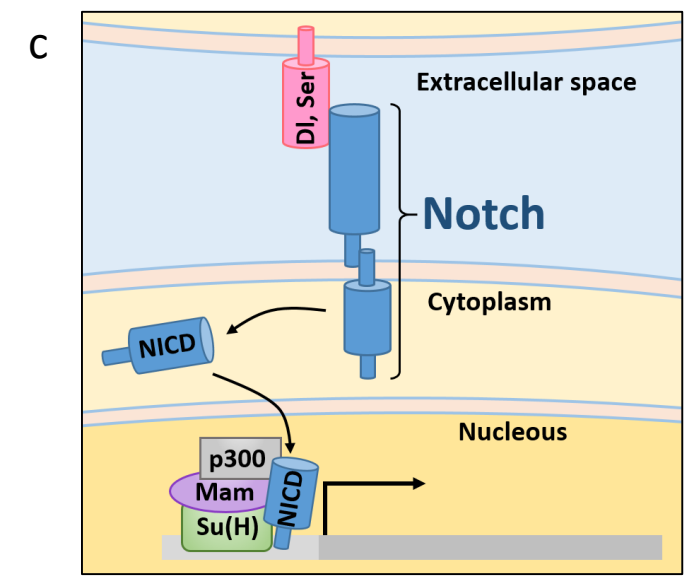
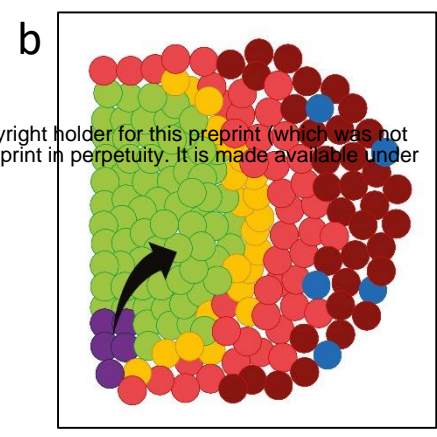
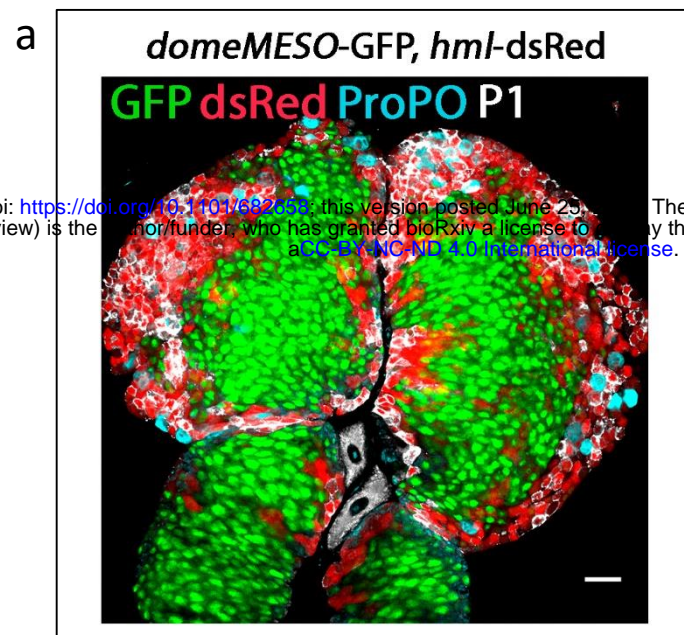


- 563 47. Terriente-Felix A, Li J, Collins S, Mulligan A, Reekie I, Bernard F, et al. Notch cooperates with  
564 Lozenge/Runx to lock haemocytes into a differentiation programme. *Development*. 2013;140(4):926-37.
- 565 48. Wilson A, MacDonald HR, Radtke F. Notch 1-deficient common lymphoid precursors adopt a B  
566 cell fate in the thymus. *J Exp Med*. 2001;194(7):1003-12.
- 567 49. Pui JC, Allman D, Xu L, DeRocco S, Karnell FG, Bakkour S, et al. Notch1 expression in early  
568 lymphopoiesis influences B versus T lineage determination. *Immunity*. 1999;11(3):299-308.
- 569 50. Evans CJ, Olson JM, Ngo KT, Kim E, Lee NE, Kuoy E, et al. G-TRACE: rapid Gal4-based cell lineage  
570 analysis in *Drosophila*. *Nat Methods*. 2009;6(8):603-5.

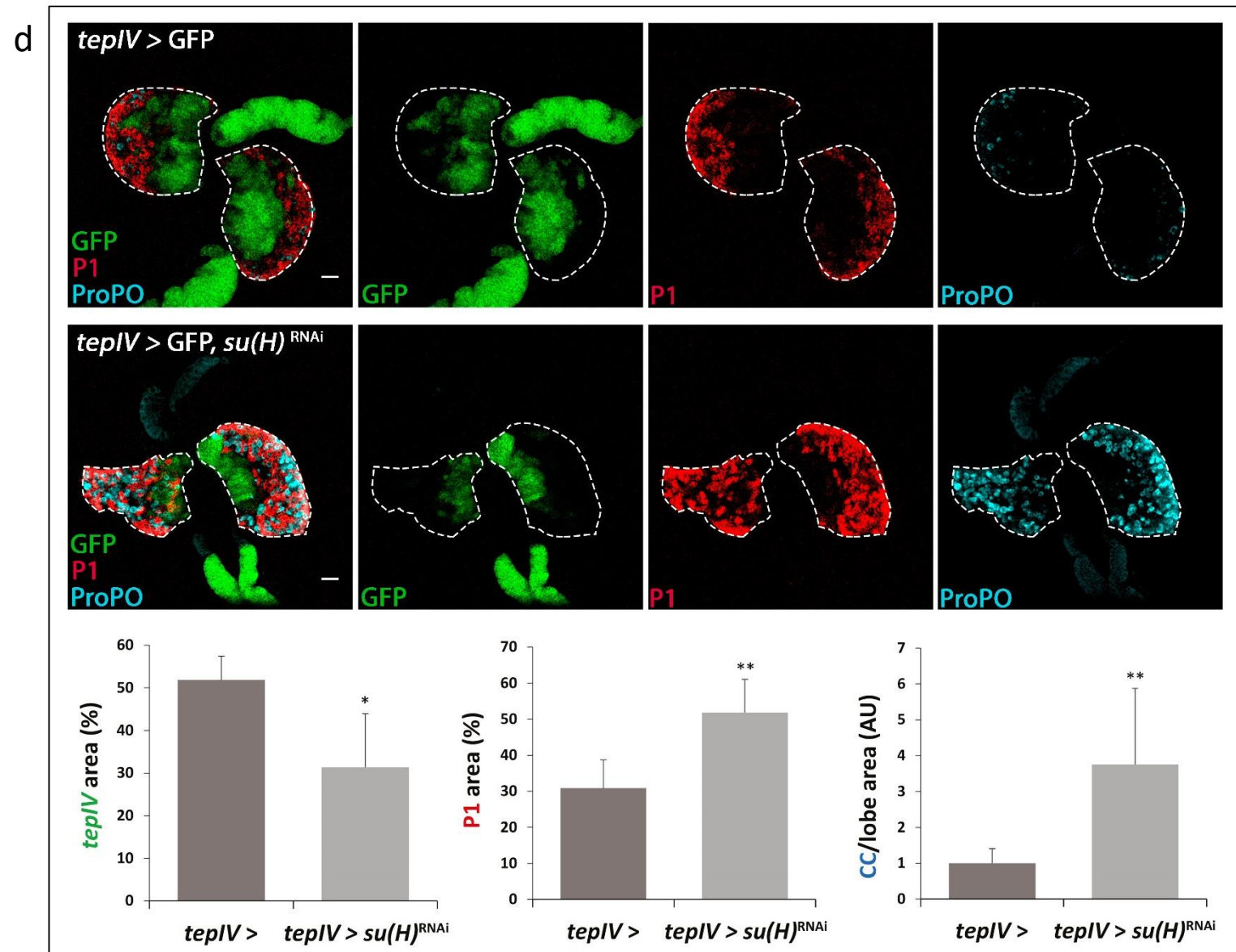
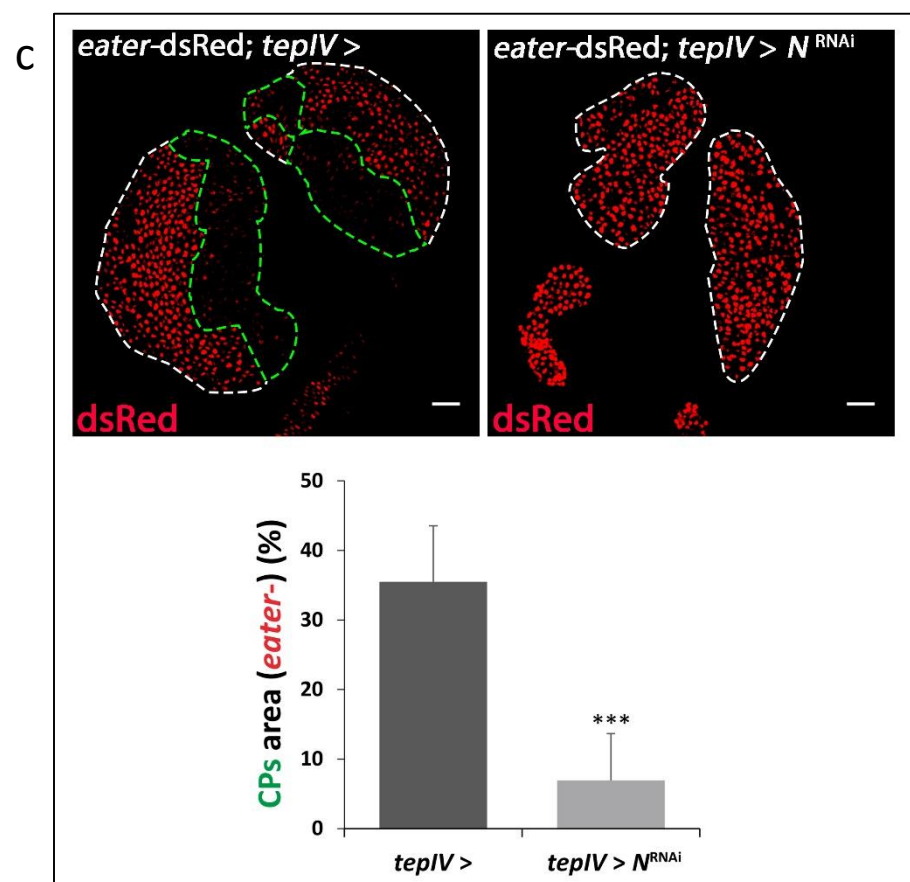
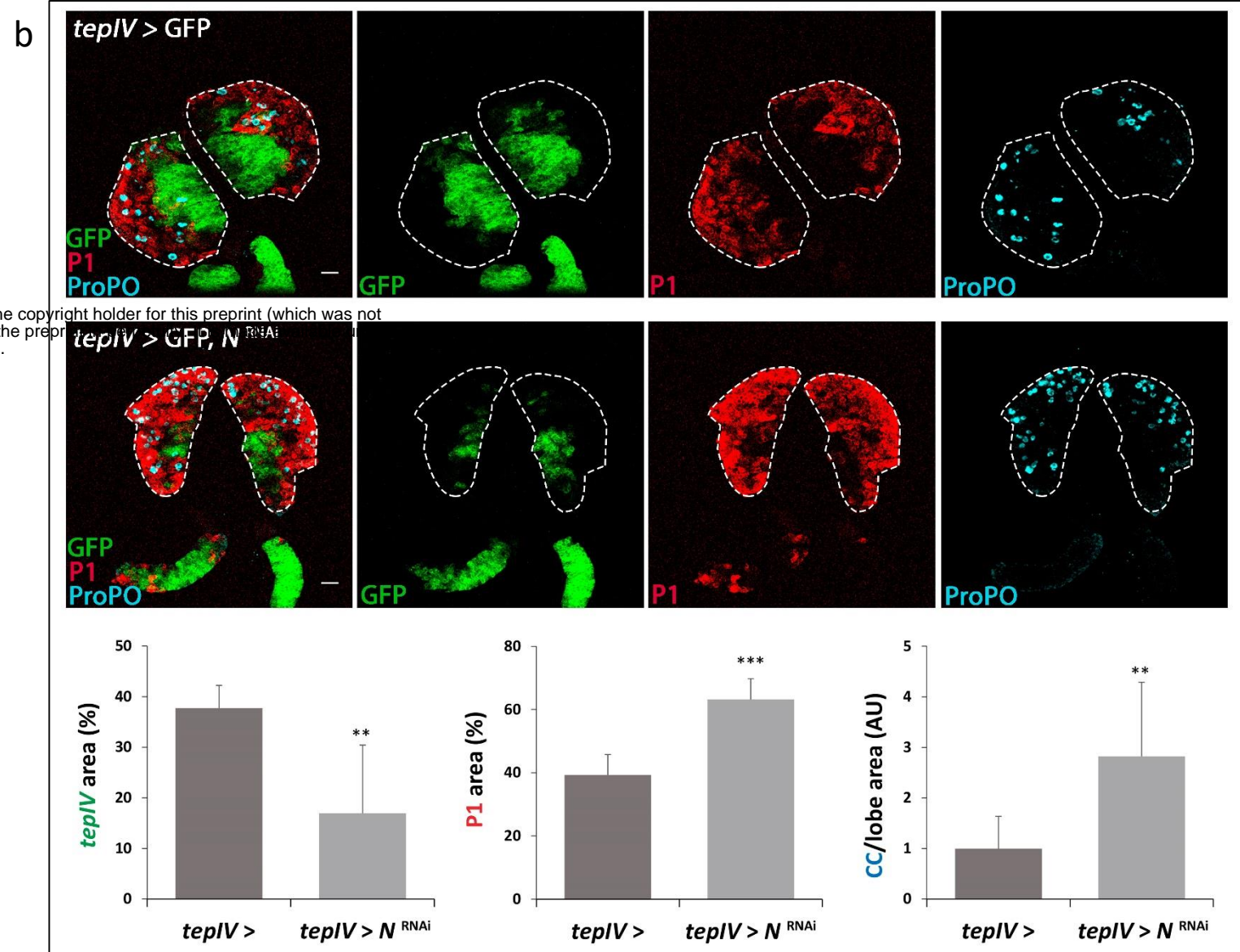
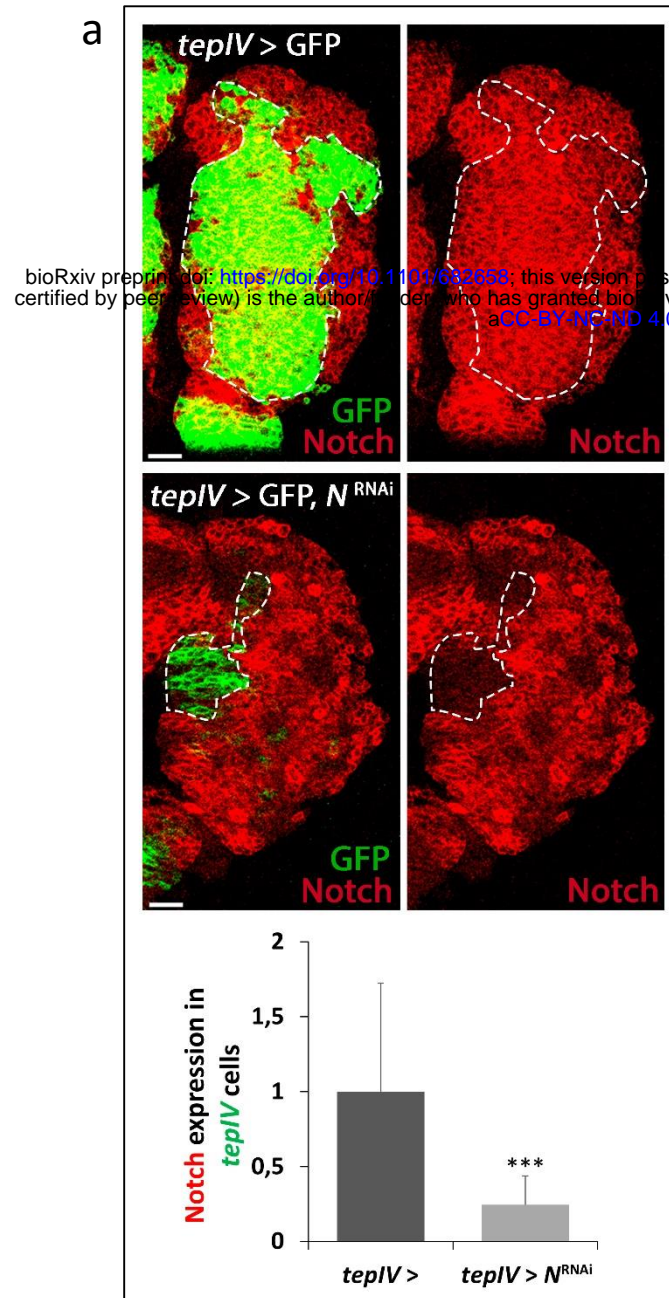
571

# Figure 1

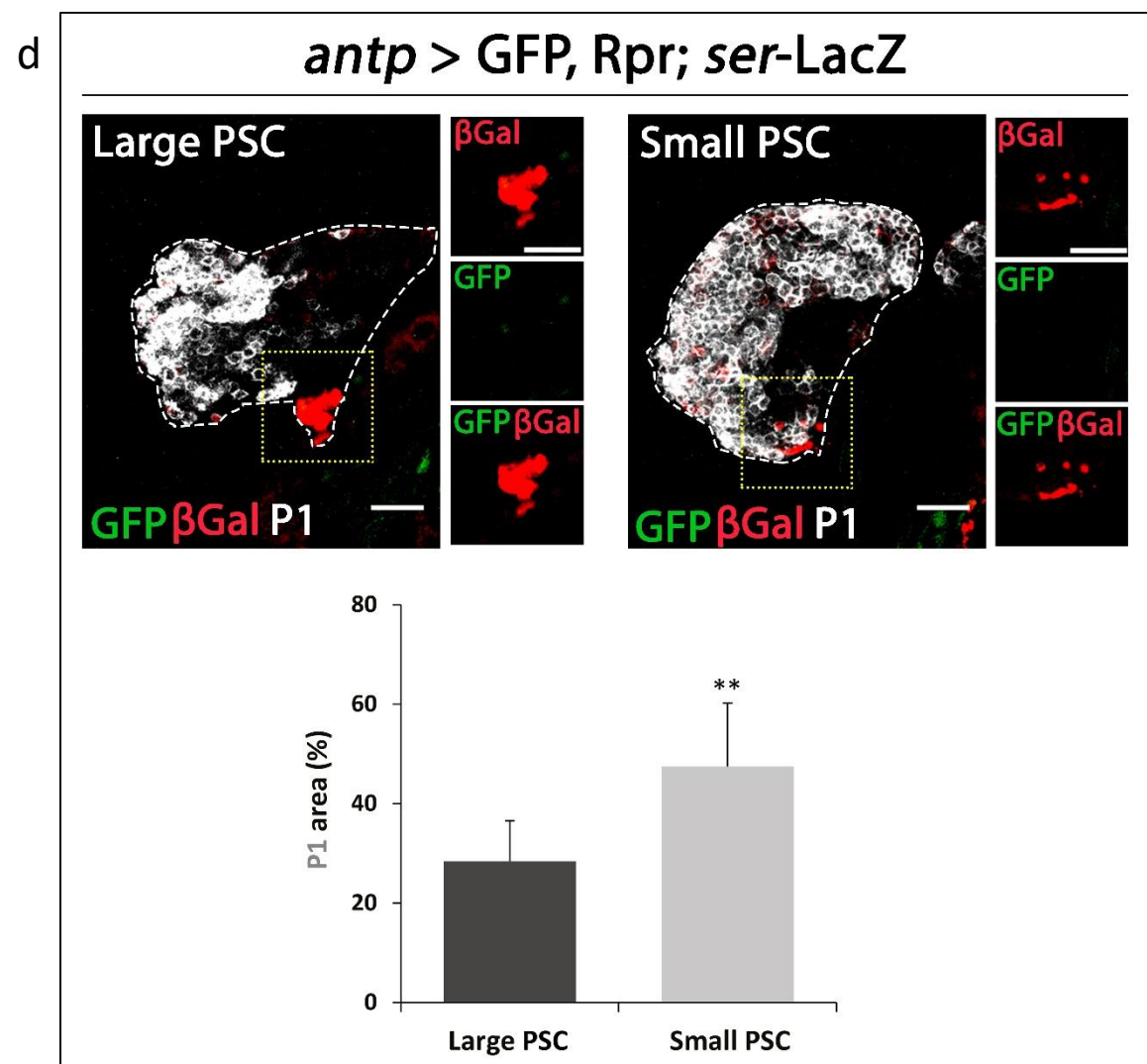
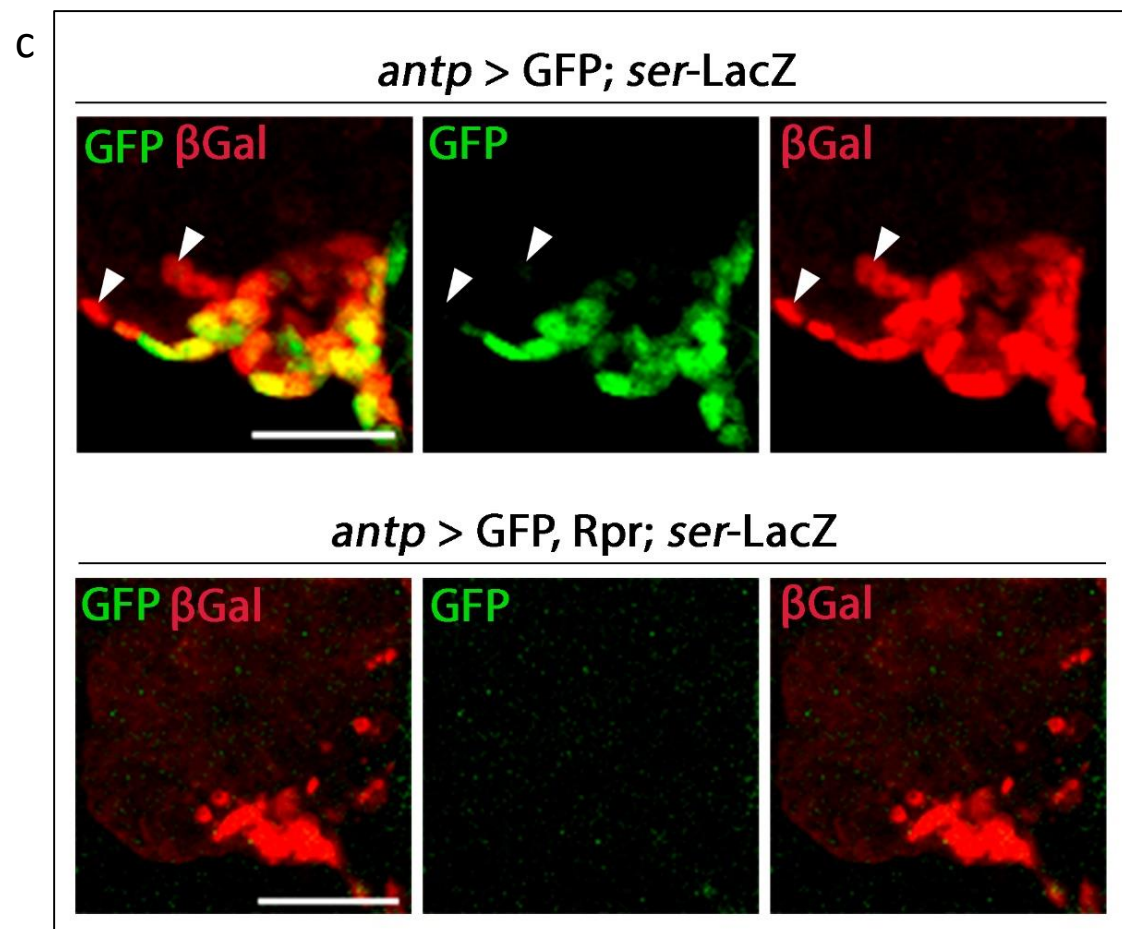
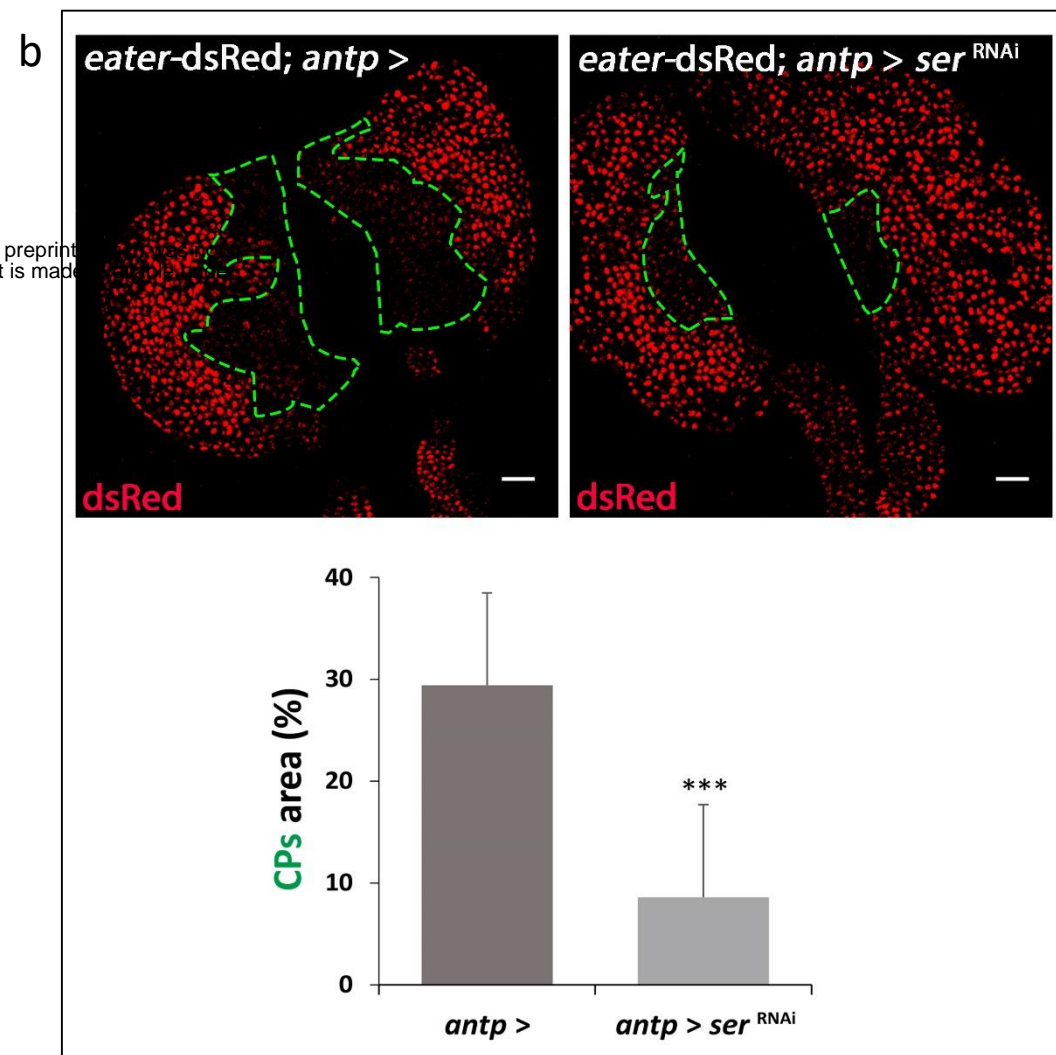
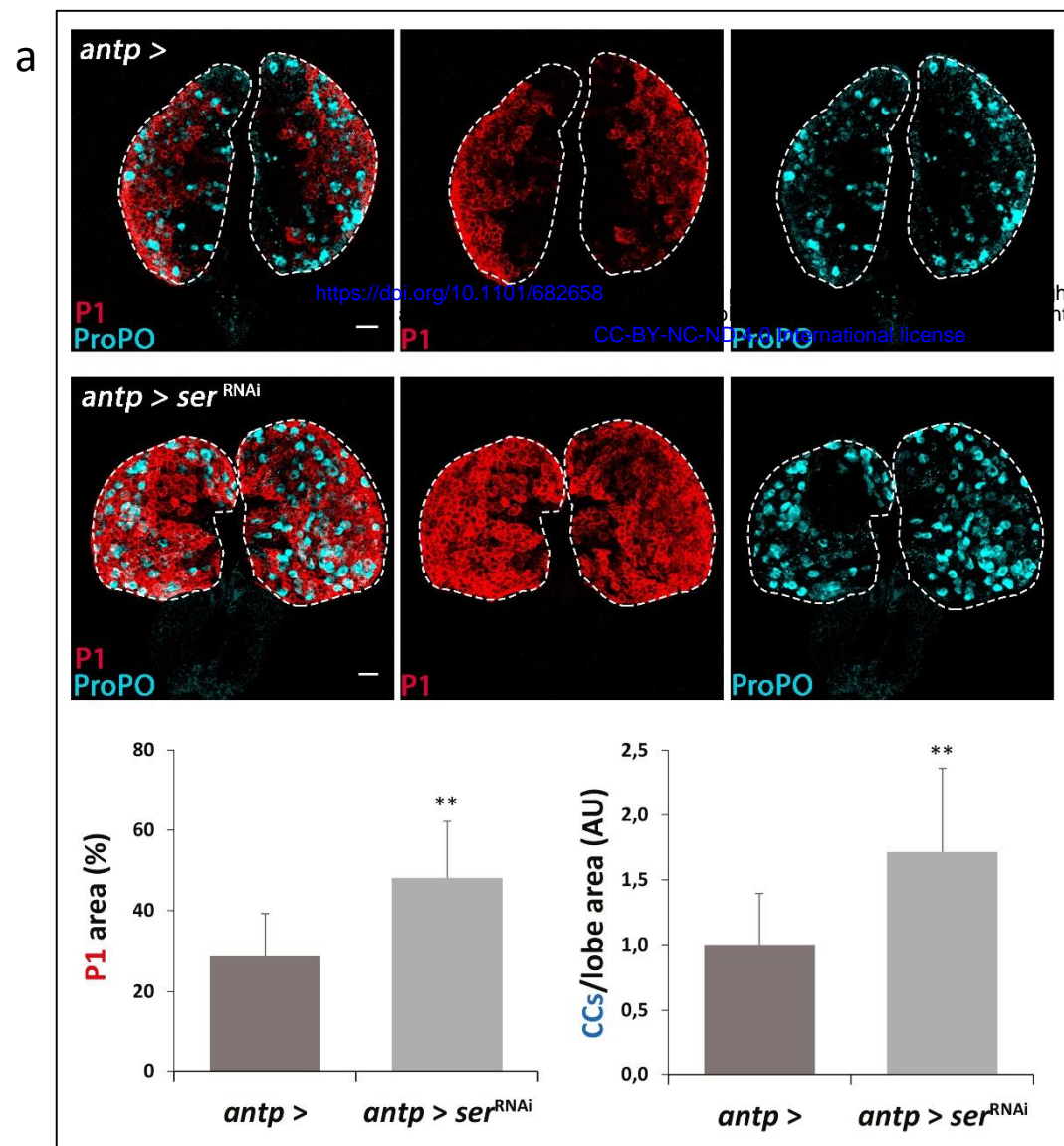
bioRxiv preprint doi: <https://doi.org/10.1101/082756>; this version posted June 29, 2016. The copyright holder for this preprint (which was not certified by peer review) is the author/funder, who has granted bioRxiv a license to display the preprint in perpetuity. It is made available under aCC-BY-NC-ND 4.0 International license.



# Figure 2



# Figure 3



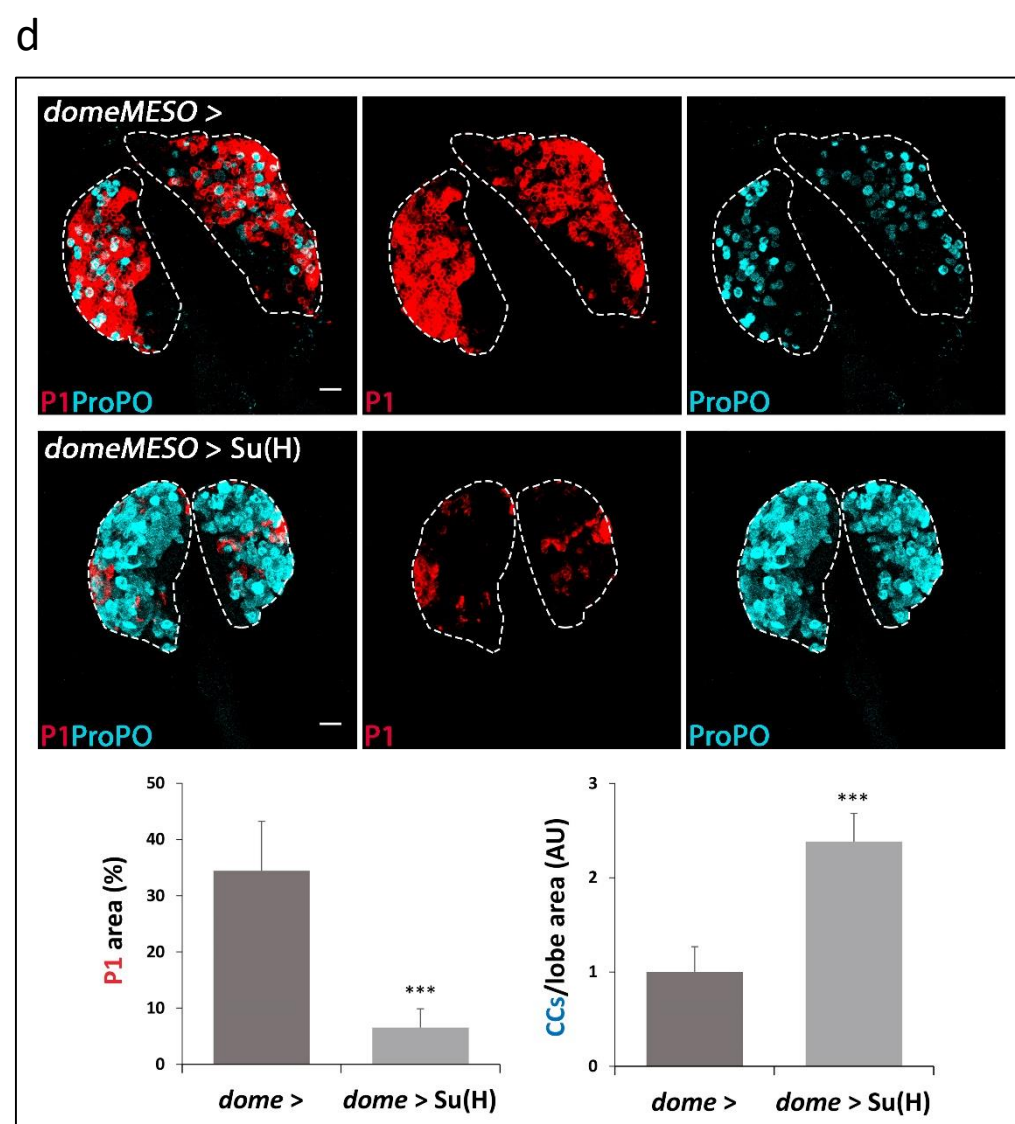
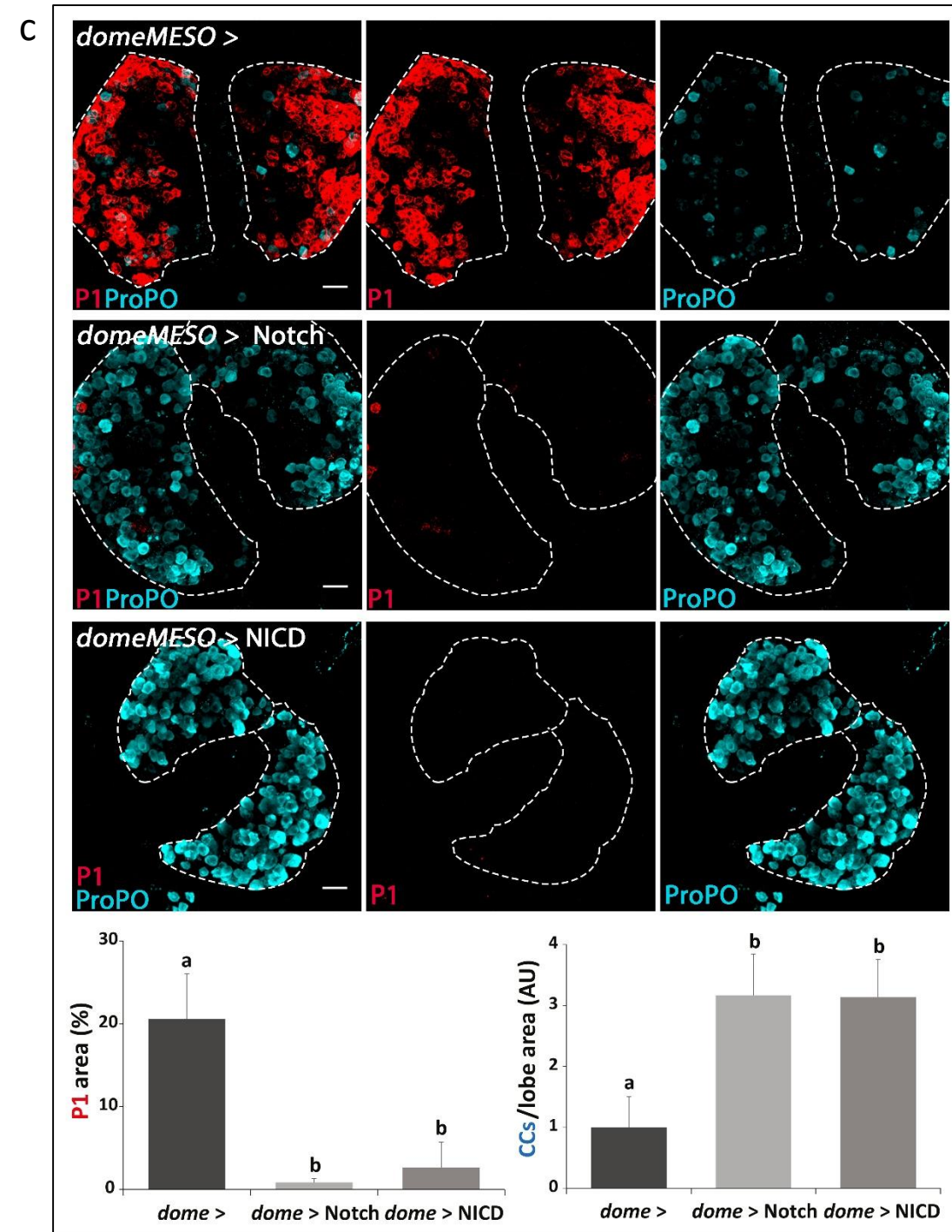
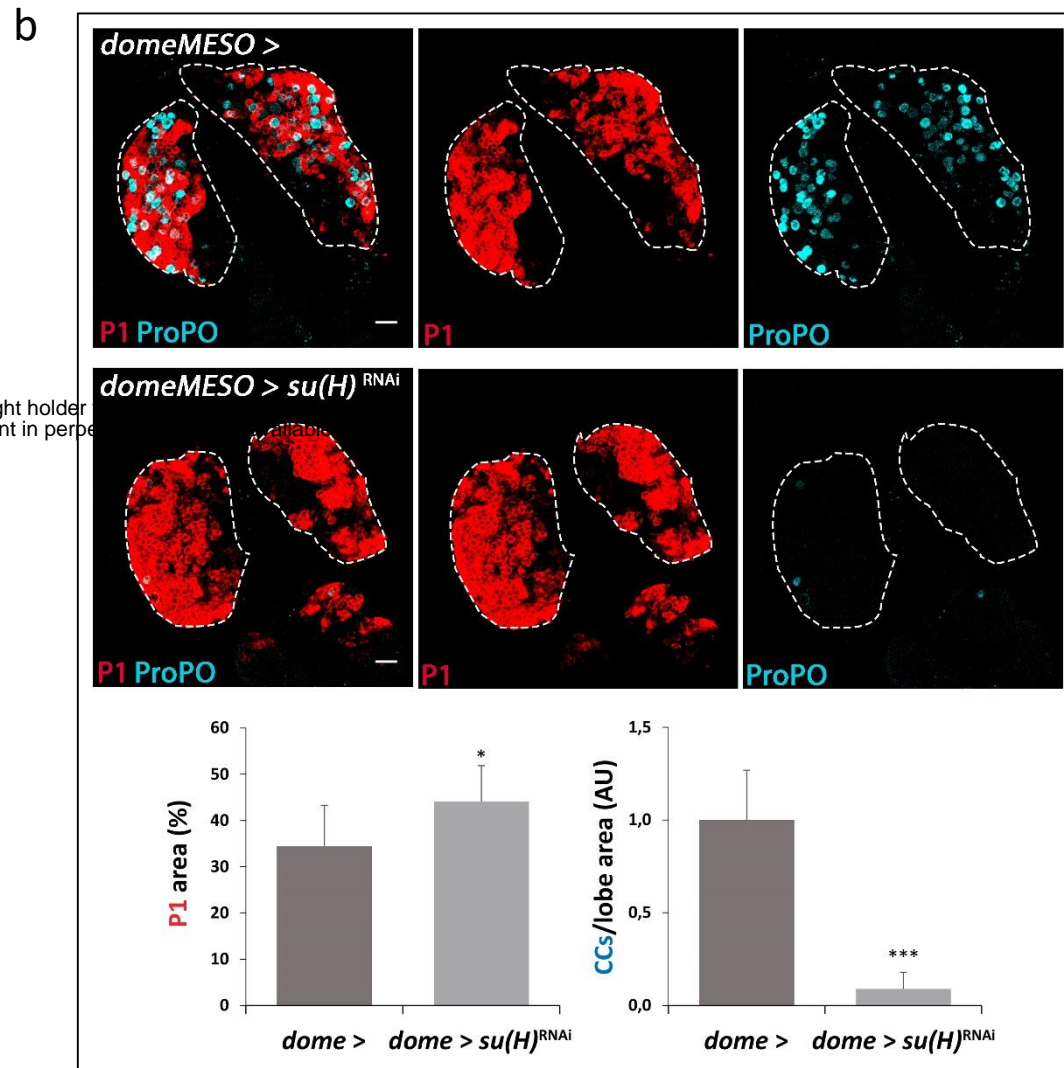
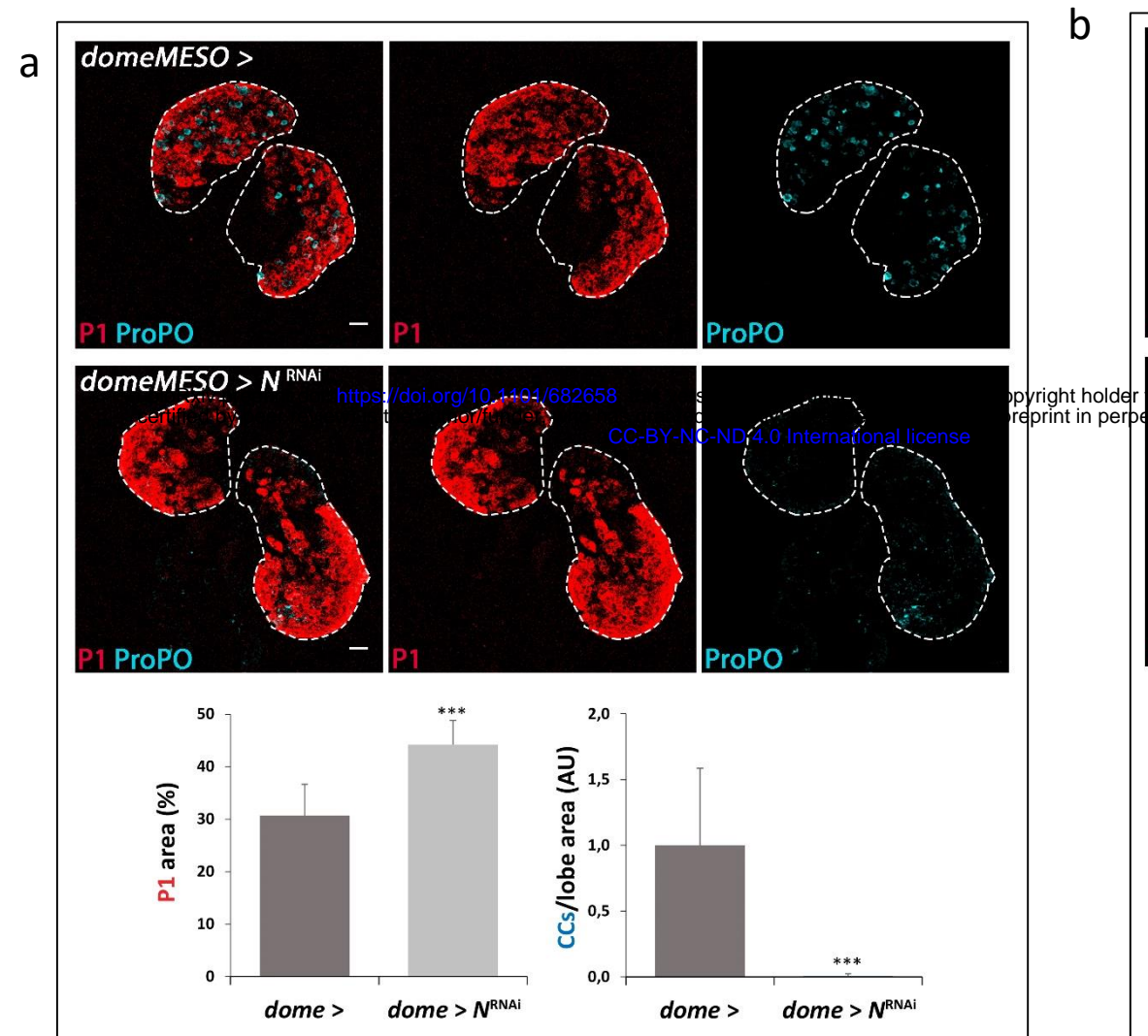


# Figure 5

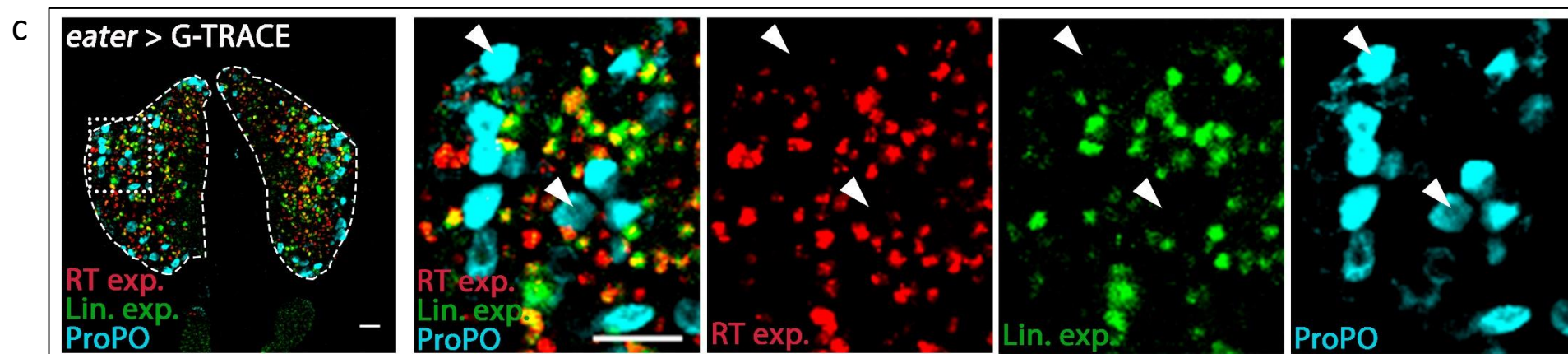
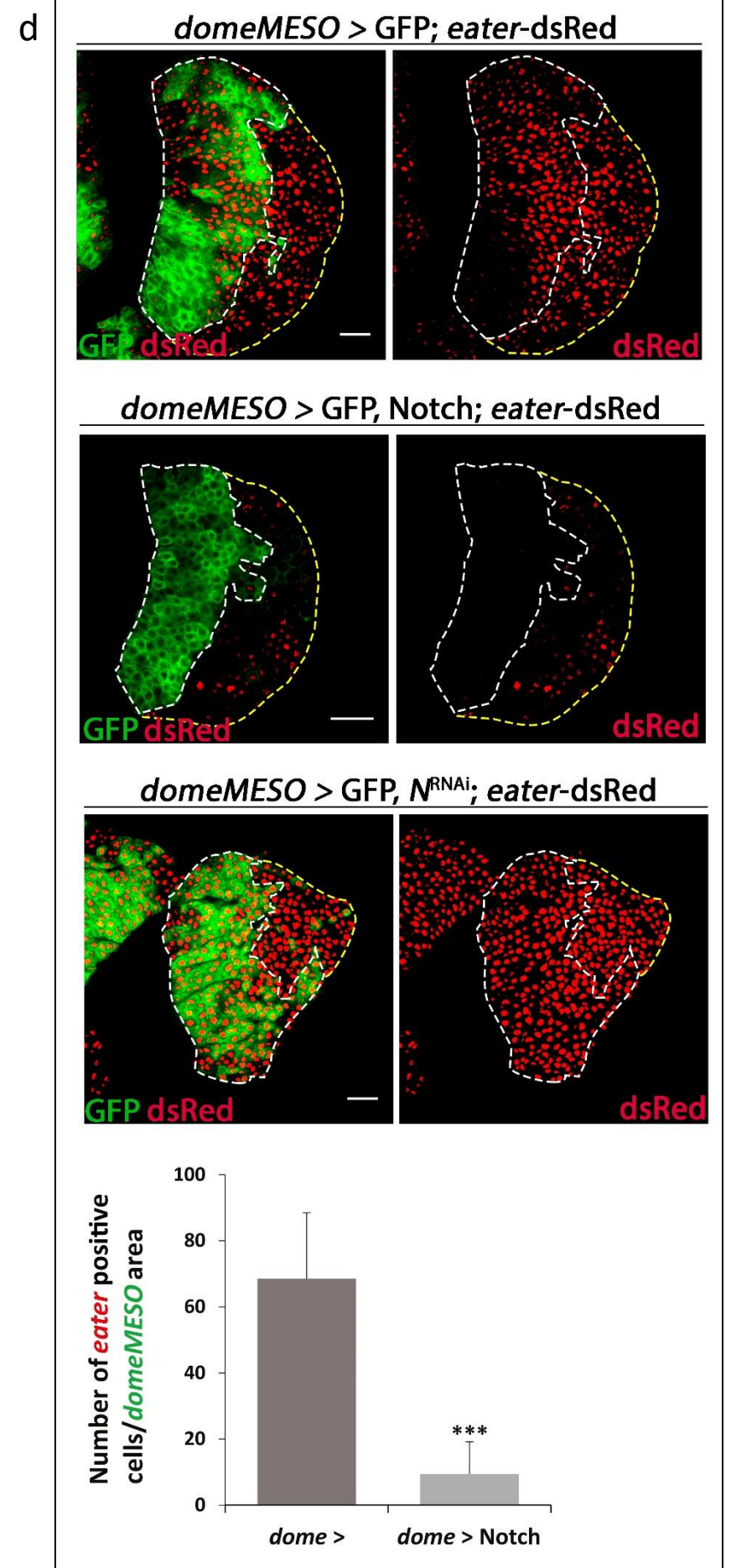
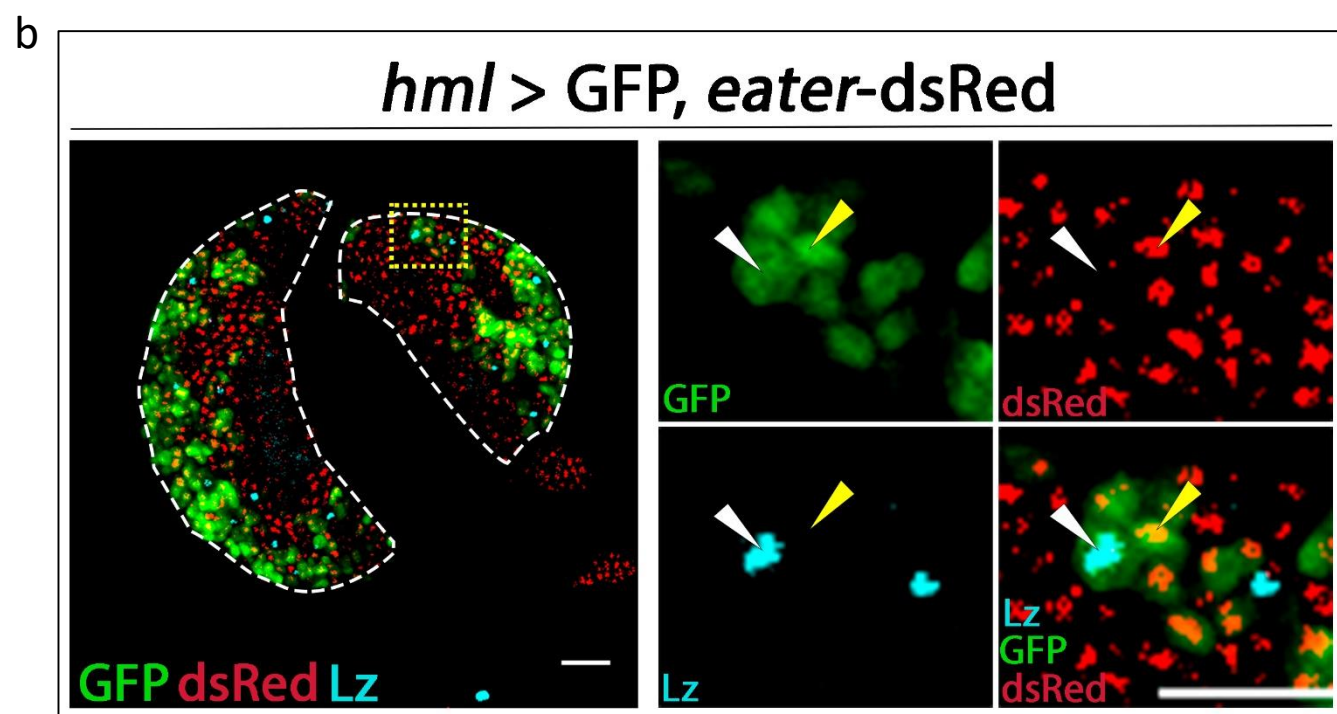
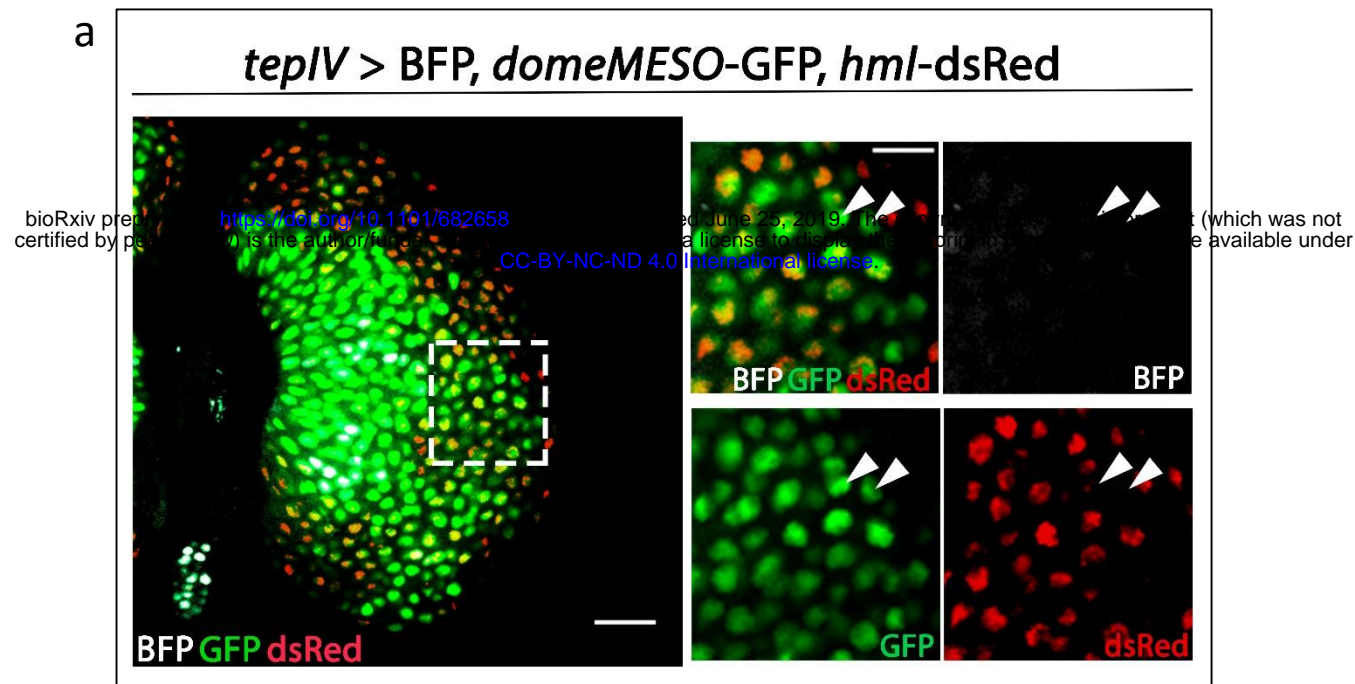


# Figure 6

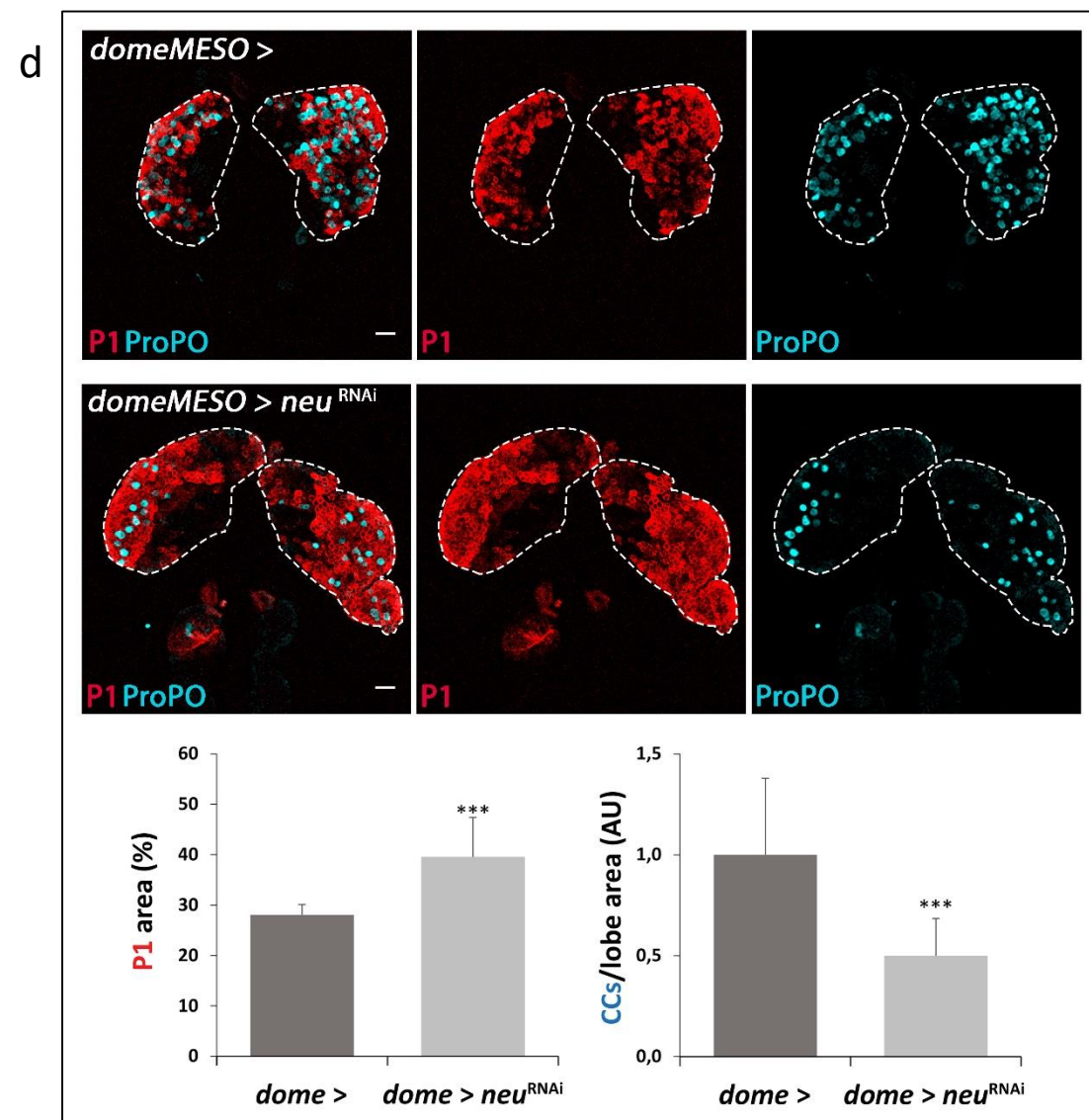
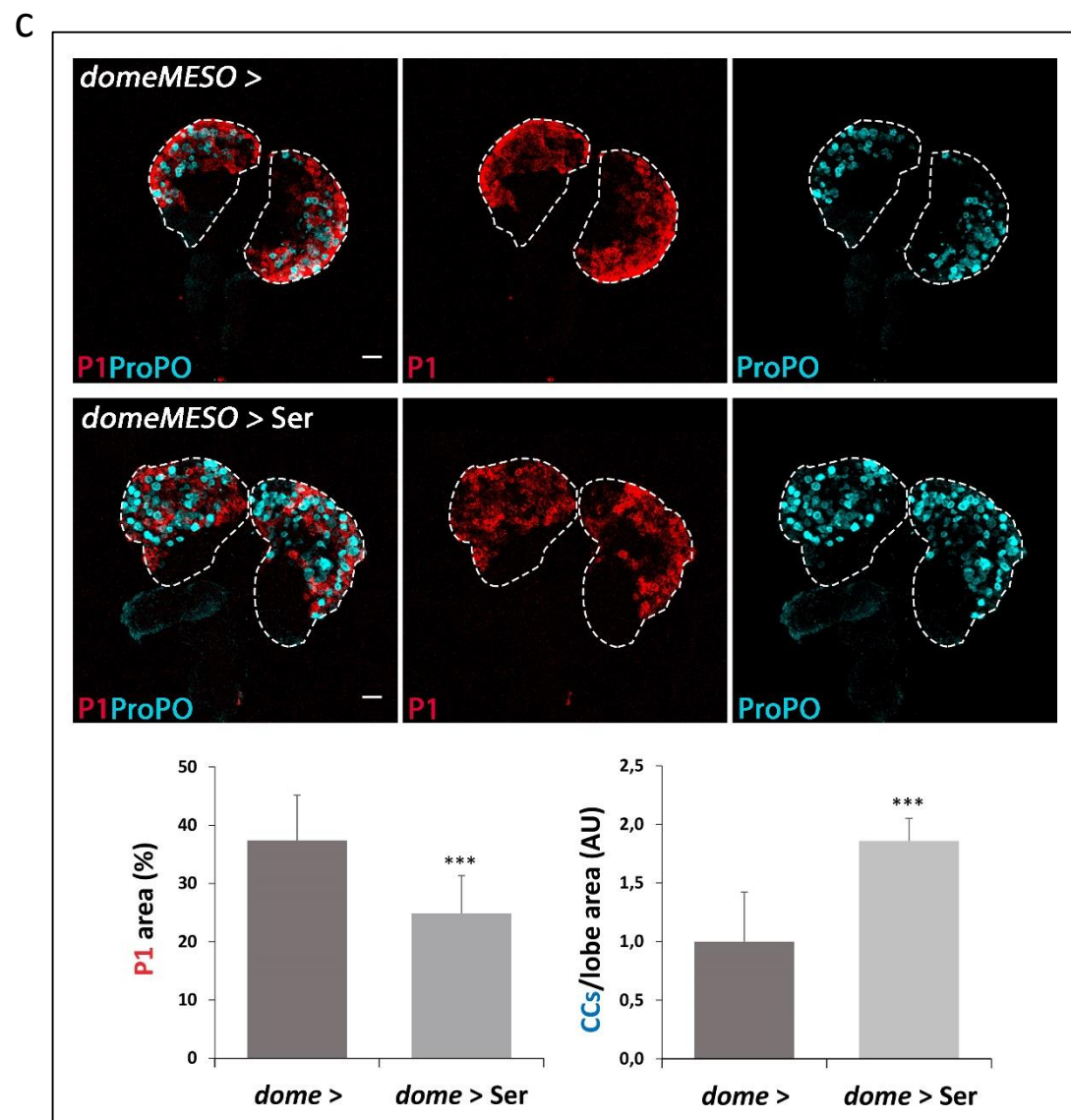
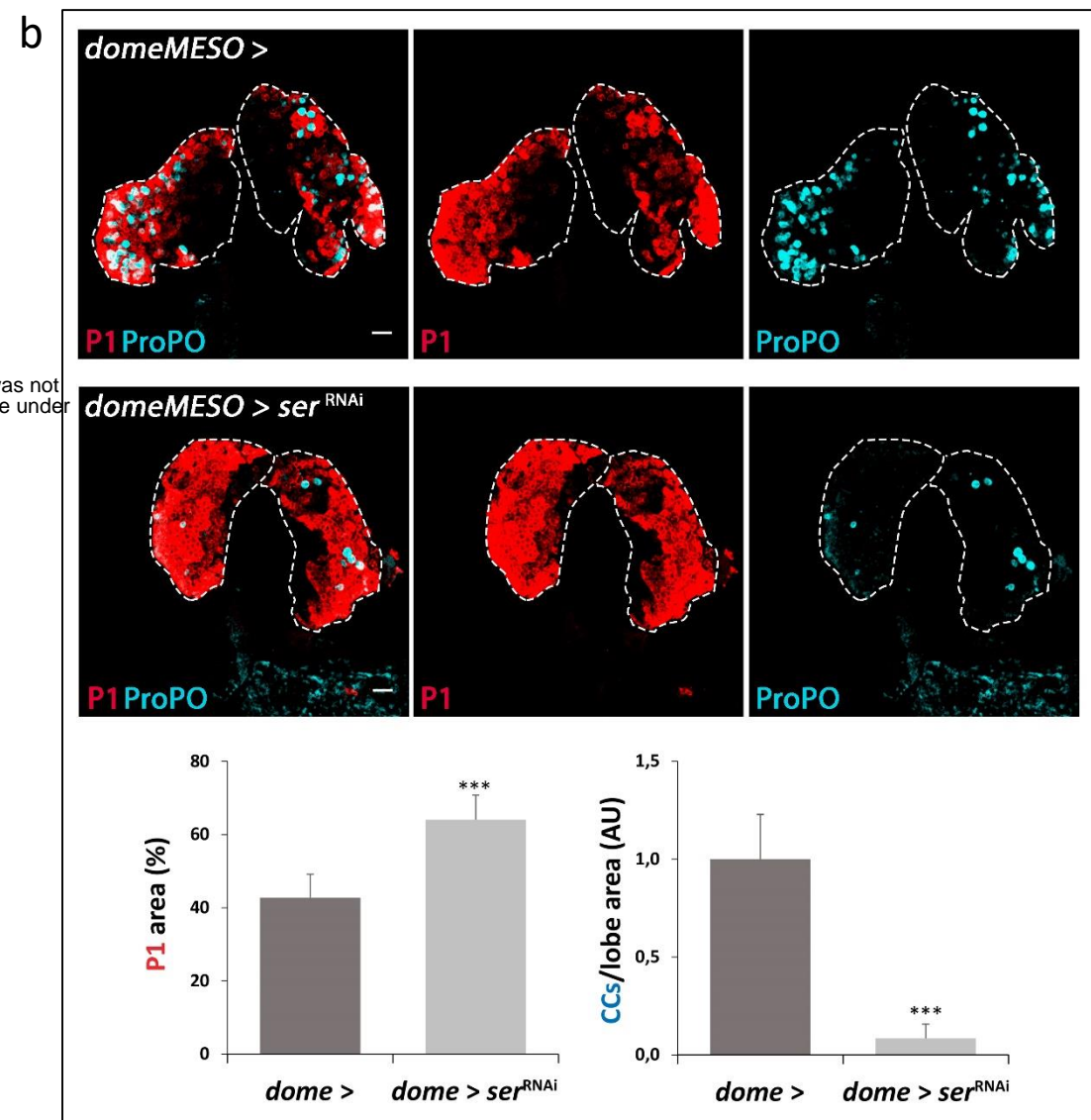
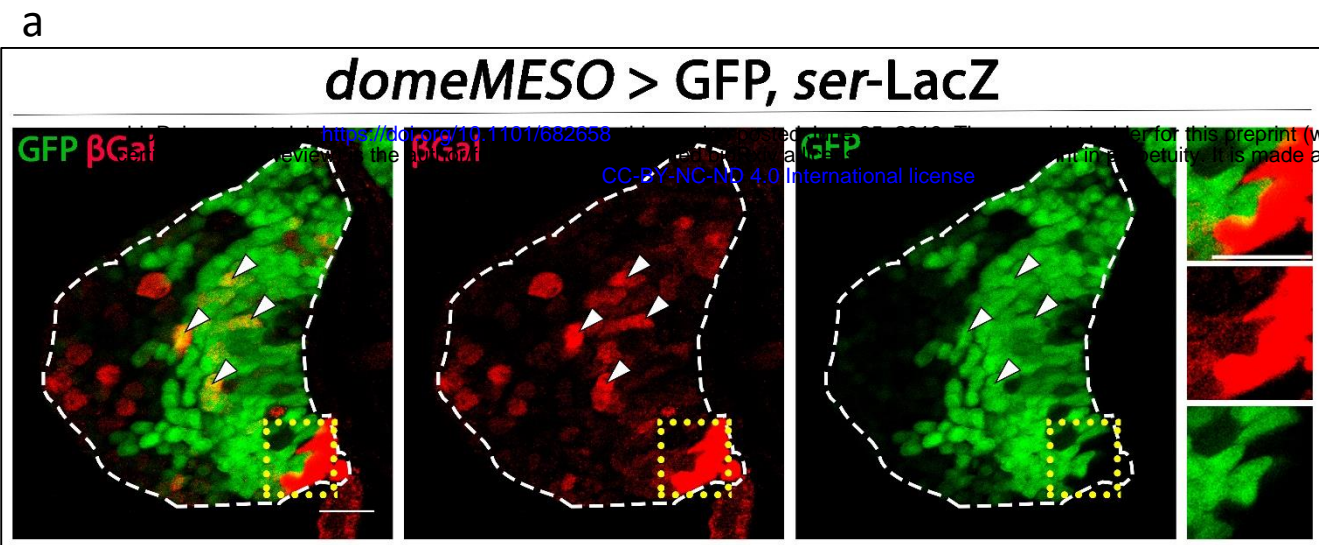
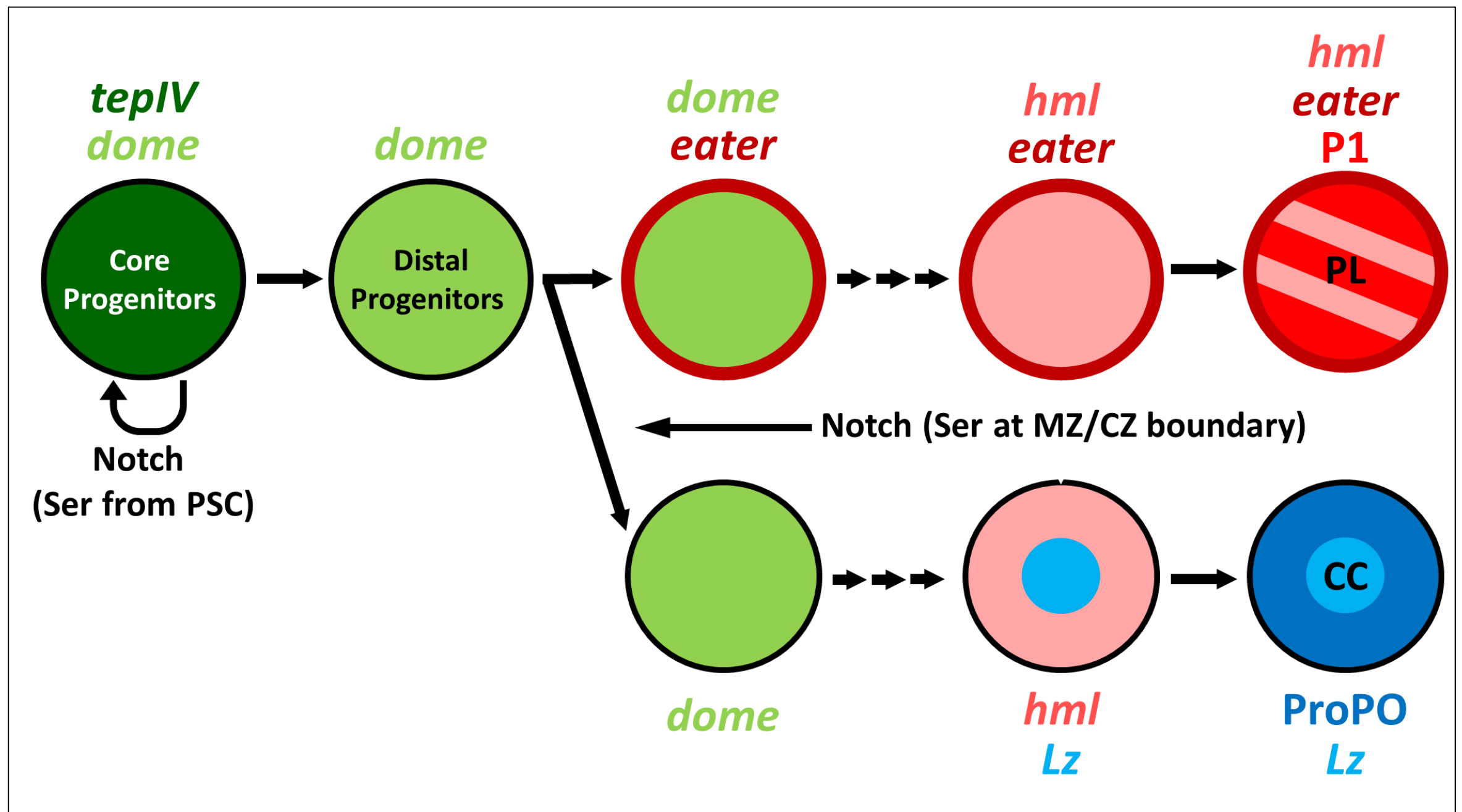


# Figure 7

bioRxiv preprint doi: <https://doi.org/10.1101/682658>; this version posted June 25, 2019. The copyright holder for this preprint (which was not certified by peer review) is the author/funder, who has granted bioRxiv a license to display the preprint in perpetuity. It is made available under aCC-BY-NC-ND 4.0 International license.





## 570 **Figure legends**

571

### 572 **Figure 1. Progenitor populations of the lymph gland**

573 **(a) Cell populations of the lymph gland.** Blood cell progenitors (green; *domeMESO*-GFP);  
574 differentiating cells (red; *hml*-dsRed); Crystal Cells (cyan, anti-ProPO staining) and  
575 Plasmatocytes (white, anti-P1 staining). Single-plane confocal images of primary lobes from  
576 wandering third instar larvae are shown. Scale bar, 20  $\mu$ m.

577 **(b) Schematic representation of a wandering 3<sup>rd</sup> instar lymph gland lobe.** Purple: Posterior  
578 Signaling Center; green: Blood cell progenitors; yellow: Intermediate Progenitors; pink:  
579 Differentiating cells; dark red: Plasmatocytes; blue: Crystal Cells. The black arrow indicates  
580 progenitor maintenance signals that emanate from the PSC.

581 **(c) Simplified scheme of the Notch pathway.** Dl: Delta, Ser: Serrate. NICD: Notch Intracellular  
582 Domain, Su(H): Suppressor of Hairless, Mam: Mastermind.

583 **(d) Three populations of blood cell progenitors occur in the lymph gland.** Region 1: Cells that  
584 express both *tepIV* > BFP (white) and *domeMESO*-GFP (green). Region 2: Cells that express  
585 *domeMESO*-GFP but not *tepIV* > BFP or *hml*-dsRed (red). Region 3: Cells in which *domeMESO*-  
586 GFP and *hml*-dsRed signals coexist. Single-plane confocal images of primary lobes from  
587 wandering third instar larvae are shown. Scale bar, 20  $\mu$ m.

588 **(e) The Plasmatocyte marker *eater* is expressed in a subpopulation of blood cell progenitors.**  
589 Progenitors that express both *tepIV* > BFP (white) and *domeMESO*-GFP (green) co-express  
590 almost undetectable levels of the plasmatocyte marker *eater*-dsRed (red) (region 1). In  
591 contrast, *eater*-dsRed expression can be readily detected in Distal Progenitors that are  
592 *domeMESO*-GFP positive and negative for *tepIV* > BFP (region 2). Single-plane confocal images  
593 of primary lobes from wandering third instar larvae are shown. Scale bar, 20  $\mu$ m.

594 **(f) Schematic representation of a wandering 3<sup>rd</sup> instar wild-type lymph gland lobe with  
595 redefined progenitor populations.** Progenitors encompass three subpopulations: 1) Core  
596 Progenitors, positive for *domeMESO* and *tepIV* (dark green); 2) Distal Progenitors, negative for  
597 *tepIV* and *hml* and positive for *domeMESO* (light green); and 3) Intermediate Progenitors,  
598 which are positive for both *domeMESO* and *hml* (yellow). The color code for the remaining cell  
599 populations are as in Fig. 1b: Purple: Posterior Signaling Center; pink: *hml*-positive  
600 differentiating cells; dark red: Plasmatocytes; blue: Crystal Cells.

601

602

### 603 **Figure 2. The Notch pathway is required for Core Progenitor maintenance.**

604 **(a) Notch is expressed throughout the lymph gland.** Staining with an anti-Notch antibody  
605 (red) in control lymph glands (upper panels), or in lymph glands expressing a *tepIV*-Gal4 driven  
606 *notch* RNAi ( $N^{RNAi}$ ) (middle panels). Single-plane confocal images of primary lobes from  
607 wandering third instar larvae are shown. Scale bars, 20  $\mu$ m. *TepIV* > GFP marks the area of Core  
608 Progenitors, which is also delimited with a white dashed line. Note that following  $N^{RNAi}$   
609 expression, Notch staining was reduced in CPs (middle panels). Lower panel: Quantification of  
610 mean anti-Notch signal levels in Core Progenitors (\*\*p < 0.001). Error bars represent SD.  
611 *tepIV* >, n = 16; *tepIV* >  $N^{RNAi}$ , n = 18.

612 **(b) Notch is required for Core Progenitor maintenance.** *Notch* RNAi ( $N^{RNAi}$ ) expression in Core  
613 Progenitors, driven by *tepIV*-Gal4, provoked loss of Core Progenitors (green: *tepIV* > GFP),  
614 along with increased Plasmatocytes (red: P1 staining) and Crystal Cells (cyan: ProPO staining).  
615 Compare control lymph glands in upper panels with lymph glands expressing  $N^{RNAi}$  in middle  
616 panels. Whole Z-projection confocal images of primary lobes from wandering third instar

617 larvae are depicted. Graphs in lower panels show quantification of the indicated markers (\*\*p  
618 < 0.01, \*\*\*p < 0.001). Error bars represent SD. *teplV* >, n = 8; *teplV* > *N<sup>RNAi</sup>*, n = 8.

619 **(c) *eater*-dsRed reporter expression domain is expanded upon Core Progenitor loss.**

620 Expression of the *eater*-dsRed reporter (red) in control lymph glands (left panel) and in lymph  
621 glands expressing *notch* RNAi (*N<sup>RNAi</sup>*) in Core Progenitors under the *teplV*-Gal4 driver (right  
622 panel). The green dashed line marks *eater*-negative Core Progenitors area. Single-plane  
623 confocal images of primary lobes from wandering third instar larvae are shown. The graph  
624 shows quantification of *eater*-negative area corresponding to Core Progenitors (\*\*\*p < 0.001).  
625 Error bars represent SD. *teplV* >, n = 8; *teplV* > *N<sup>RNAi</sup>*, n = 15.

626 **(d) Suppressor of Hairless (Su(H)) is required for Core Progenitor maintenance.** *Su(H)<sup>RNAi</sup>*

627 expression with *teplV*-Gal4 caused a reduction of Core Progenitors (green: *teplV* > GFP), and a  
628 simultaneous increase of Plasmatocytes (red: P1 staining) and Crystal Cells (cyan: ProPO  
629 staining). Upper panels: Controls without RNAi; Middle panels: Expression of *su(H)<sup>RNAi</sup>*. Whole  
630 Z-projection confocal images of primary lobes from wandering third instar larvae are depicted.  
631 Graphs in lower panels show quantification of the indicated markers (\*p < 0.05, \*\*p < 0.01).  
632 Error bars represent SD. *teplV* >, n = 8; *teplV* > *su(H)<sup>RNAi</sup>*, n = 5.

633

634

635 **Figure 3. Serrate is required at the Posterior Signaling Center for Core Progenitor**  
636 **maintenance.**

637 **(a) *Serrate* (*Ser*) silencing at the Posterior Signaling Center provokes increased differentiation**

638 **of Plasmatocytes and Crystal Cells.** Following *serrate* RNAi (*ser<sup>RNAi</sup>*) expression with an *antp*-  
639 Gal4 driver, a general increase of cell differentiation was observed. Plasmatocytes are in red  
640 (P1 staining) and Crystal Cells in cyan (ProPO staining). Upper panels: Control lymph glands;  
641 middle panels: Lymph glands with expression of *ser<sup>RNAi</sup>* driven by *antp*-Gal4. Whole Z-  
642 projection confocal images of primary lobes from wandering third instar larvae are shown.  
643 Scale bars, 20  $\mu$ m. Lower panels: Quantification of the results (\*\*p < 0.01). Error bars  
644 represent SD. *Antp* >, n = 10; *antp* > *ser<sup>RNAi</sup>*, n = 14.

645 **(b) *Serrate* (*ser*) silencing at the Posterior Signaling Center provokes a reduction of Core**

646 **Progenitors.** Expression of the *eater*-dsRed reporter is shown, and the area that lacks its  
647 expression corresponds to Core Progenitors (marked with green dashed lines). Left panel:  
648 Control Lymph gland; right panel: Lymph gland with *ser* silencing at the Posterior Signaling  
649 Center. Single-plane confocal images of primary lobes from wandering third instar larvae are  
650 shown. Scale bars, 20  $\mu$ m. Lower panel: quantification of the area occupied by *eater*-negative  
651 Core Progenitors. Error bars represent SD. *Antp* >, n = 14; *antp* > *ser<sup>RNAi</sup>*, n = 19.

652 **(c) *Serrate*-expressing cells of the Posterior Signaling Center survive to genetic ablation of**

653 ***antennapedia*-expressing cells.** *Antennapedia* (*antp*)-positive cells of the Posterior Signaling  
654 Center (PSC) are visualized with *antp*-Gal4 driven expression of GFP (*antp* > GFP, green), while  
655 *serrate* (*ser*) expressing cells are shown with anti- $\beta$ Gal staining (red) of *ser*-LacZ reporter.  
656 Expression of the pro-apoptotic protein Reaper (Rpr) with an *antp*-Gal4 driver from L2 stage  
657 onwards (see text) eliminates all *antp*-positive cells, but many *ser* expressing cells survive.  
658 Upper panels: control lymph glands without Rpr expression. The wild-type PSC comprises a  
659 mixed population of *antp* and *ser* double-positive cells (*ser<sup>+</sup>, antp<sup>+</sup>*) and *ser* positive-*antp*  
660 negative cells (*ser<sup>+</sup>, antp<sup>-</sup>*) (examples of the latter are shown with arrowheads); lower panels:  
661 lymph glands expressing Rpr under *antp*-Gal4. After genetic ablation, all of the observed PSC  
662 cells express *ser* and lack *antp* expression. Single-plane confocal images of the PSC region of  
663 primary lobes from wandering third instar larvae are shown. Scale bars, 20  $\mu$ m.

664 **(d) After *antennapedia*-Gal4 driven genetic ablation, the abundance of the surviving *serrate*-**  
665 **expressing cells of the Posterior Signaling Center correlates negatively with the amount of**  
666 **Plasmatocytes.** In lymph glands in which *antp*-expressing cells of the Posterior Signaling Center  
667 (PSC) have been ablated by *antp*-Gal4 driven expression of Reaper (Rpr), Plasmatocytes  
668 differentiation (white, P1 staining) correlates negatively with the area occupied by *serrate*-LacZ  
669 expressing cells that survived genetic ablation (red,  $\beta$ Gal staining). Examples of large and small  
670 *ser*-positive PSC areas are shown (“Large PSC” on the left panel and “Small PSC” on the right  
671 panel, respectively). Inset shows a magnification of the PSC region, with all cells of the PSC  
672 expressing *ser* but not *antp*. Whole Z-projection confocal images of primary lobes from  
673 wandering third instar larvae are depicted. Scale bars, 20  $\mu$ m. The graph shows quantification  
674 of P1-positive area in *antp*-ablated lymph glands that exhibit large or small PSC area. PSC area  
675 was considered small if it was less than %1.5 of the total lobe area). Large PSC, n = 7, Small  
676 PSC, n = 8.

677  
678

679 **Figure 4. Notch regulates the Plasmatocyte/Crystal Cell fate decision in Distal Progenitors.**

680 **(a) *Notch* (*N*) silencing in *domeMESO*-positive progenitors abolishes Crystal Cell specification**  
681 **and promotes the Plasmatocyte cell fate.** *Notch* RNAi ( $N^{RNAi}$ ) expression with the *domeMESO*-  
682 Gal4 driver provoked loss of Crystal Cells (cyan: ProPO staining), along with increased  
683 Plasmatocytes (red: P1 staining). Compare control lymph glands in upper panels with lymph  
684 glands expressing  $N^{RNAi}$  in middle panels. Whole Z-projection confocal images of primary lobes  
685 from wandering third instar larvae are displayed. Charts in lower panels show quantification of  
686 the indicated markers (\*\* $p < 0.001$ ). Error bars represent SD. *dome* >, n = 8; *dome* >  $N^{RNAi}$ , n =  
687 8.

688 **(b) *Suppressor of hairless* (*su(H)*) silencing in *domeMESO*-positive progenitors is similar to**  
689 ***notch* silencing.** *Su(H)* RNAi ( $su(H)^{RNAi}$ ) expression with the *domeMESO*-Gal4 driver provoked  
690 loss of Crystal Cells (cyan: ProPO staining) and increased Plasmatocytes (red: P1 staining).  
691 Upper panels: control lymph glands; middle panels: lymph glands expressing  $su(H)^{RNAi}$ . Whole  
692 Z-projection confocal images of primary lobes from wandering third instar larvae are shown.  
693 Lower panels: quantification of the indicated markers (\* $p < 0.05$ , \*\* $p < 0.001$ ). Error bars  
694 represent SD. *dome* >, n = 10; *dome* >  $su(H)^{RNAi}$ , n = 14.

695 **(c) Increased Notch activity in *domeMESO*-positive progenitors favors the Crystal Cell fate**  
696 **and inhibits the Plasmatocyte fate.** Full-length Notch (Notch) or the Notch Intracellular  
697 Domain (NICD) were over-expressed with a *domeMESO*-Gal4 driver. In the upper panels, a  
698 control lymph gland is shown. In the rows below lymph glands overexpressing Notch (2<sup>nd</sup> row)  
699 or NICD (3<sup>rd</sup> row) are shown. Whole Z-projection confocal images of primary lobes from  
700 wandering third instar larvae are depicted. Bottom row: Quantification of the results. Different  
701 letters indicate statistical difference (Tukey’s multiple comparison test). Error bars represent  
702 SD. *dome* >, n = 6; *dome* > Notch, n = 6; *dome* > NICD, n = 4.

703 **(d) Over-expression of *Suppressor of Hairless* (*Su(H)*) in *domeMESO*-positive progenitors**  
704 **provokes reduction of Plasmatocytes and increase of Crystal Cells, similarly to Notch over-**  
705 **expression.** Plasmatocytes are visualized in red (P1 staining) and Crystal Cells in cyan (ProPO  
706 staining). Upper panels: Control lymph glands; middle panels: Lymph glands with *domeMESO*-  
707 Gal4 driven over-expression of *Su(H)*. Whole Z-projection confocal images of primary lobes  
708 from wandering third instar larvae are displayed. Scale bar, 20  $\mu$ m. Lower panels:  
709 Quantification of the results (\*\* $p < 0.001$ ). Error bars represent SD. *dome* >, n = 7; *dome* >  
710 *Su(H)*, n = 8.

711

712 **Figure 5. Eater is an early Plasmatocyte fate marker in Distal Progenitors.**

713 **(a) Eater is expressed in all but a few Distal Progenitors of wandering 3<sup>rd</sup> instar lymph glands.**

714 Pictures show a magnification of the Region 2 of Fig. 1e, which corresponds to the Distal  
715 Progenitor region that expresses the *domeMESO*-GFP reporter (green), but lacks *tepIV*-Gal4  
716 driven BFP expression (*tepIV* > BFP, white). *Eater*-dsRed reporter (red) is expressed at high  
717 levels in most of Distal Progenitors, with exception of a few cells that show reduced or null  
718 levels (examples depicted with arrowheads). Single-plane confocal images of primary lobes  
719 from wandering third instar larvae are shown. Scale bar, 10  $\mu$ m.

720 **(b) In the Cortical Zone, the few differentiating cells that do not express *eater* are Crystal Cell**

721 **Progenitors.** Lozenge (Lz) staining (cyan) and *eater*-dsRed expression (red) is shown in lymph  
722 glands that also express GFP under *hml*-Gal4 control (*hml* > GFP, green). Inset shows an  
723 example of an *hml* > GFP positive cell that expresses the CC Progenitor marker Lz (white  
724 arrowhead), and another example of a *hml* > GFP positive cell that expresses *eater*-dsRed  
725 (yellow arrowhead). The Lz-expressing CC Progenitor lacks *eater*-dsRed expression (white  
726 arrowhead). Single-plane confocal images of primary lobes from wandering third instar larvae  
727 are shown. Scale bar, 20  $\mu$ m.

728 **(c) Eater is never expressed during Crystal Cell development.** *Eater*-Gal4 driver was used to

729 express the G-TRACE system, which allows real time and lineage detection of the expression of  
730 the Gal4 driver of interest. Crystal Cells are visualized with ProPO staining (cyan), and display  
731 neither real time (RT exp., red) nor lineage expression (Lin exp., green) of the *eater*-Gal4 driver  
732 (two examples are indicated by arrowheads). Single-plane confocal images of primary lobes  
733 from wandering third instar larvae are shown. Scale bar, 20  $\mu$ m.

734 **(d) Notch regulates Eater expression in *domeMESO*-positive cells.** *Eater*-dsRed reporter  
735 expression (red) is shown for control lymph glands (upper panels), and for lymph glands with  
736 *domeMESO*-Gal4 driven over-expression of Notch (2<sup>nd</sup> row panels) or *domeMESO*-Gal4 driven  
737 silencing of *notch* (3<sup>rd</sup> row panels). *DomeMESO*-positive cells are shown by *domeMESO*-Gal4  
738 driven expression of GFP (*domeMESO* > GFP, green). Notch over-expression with *domeMESO*-  
739 Gal4 dramatically reduces *eater*-dsRed expression in all *domeMESO*-positive cells, while *notch*  
740 RNAi (*N<sup>RNAi</sup>*) expression with *domeMESO*-Gal4 provokes that all *domeMESO*-positive cells  
741 express *eater*-dsRed. Single-plane confocal images of primary lobes from wandering third  
742 instar larvae are shown. Scale bar, 20  $\mu$ m. Lower panel: Quantification of double positive  
743 *dome*<sup>+</sup>, *eater*<sup>+</sup> cells in control and Notch over-expressing lymph glands (\*\*\*)  $p < 0.001$ . Error  
744 bars represent SD. *Dome* >, n = 9; *dome* > Notch, n = 9.

745

746

747 **Figure 6. Serrate expressed at the MZ/CZ boundary regulates the Plasmatocyte/Crystal Cell**  
748 **fate in Decision Progenitors.**

749 **(a) A fraction of *ser*-expressing cells at the MZ/CZ boundary expresses *domeMESO*.** *Ser*-

750 positive cells are visualized with  $\beta$ Gal staining (red) of the *ser*-LacZ reporter. *DomeMESO*-Gal4  
751 driver expression of GFP (*domeMESO* > GFP, green) is observed in a proportion of *ser*-  
752 expressing cells at the MZ/CZ boundary (examples are shown with arrowheads). The yellow  
753 dashed line marks the Posterior Signaling Center area. On the right, a magnification of this area  
754 shows that *ser* is also expressed in these cells, but in this case *domeMESO* is not co-expressed.  
755 Single-plane confocal images of a primary lymph gland lobe from mid-3<sup>rd</sup> instar larvae are  
756 shown. Scale bar, 20  $\mu$ m.

757 **(b) Serrate (Ser) at the Medullary Zone is required for Crystal Cell differentiation and**

758 **Plasmatocyte fate inhibition.** Plasmatocytes are visualized in red (P1 staining) and Crystal Cells  
759 in cyan (ProPO staining), in control lymph glands (upper panels) and in lymph glands that

760 express a *ser* RNAi (*ser*<sup>RNAi</sup>) under *dome*MESO-Gal4 driver control (middle panels). Whole Z-  
761 project confocal images of primary lobes from wandering third instar larvae are shown. Scale  
762 bar, 20  $\mu$ m. Lower panels: Quantification of the results (\*\*p < 0.001). Error bars represent SD.  
763 *dome* >, n = 10; *dome* > *ser*<sup>RNAi</sup>, n = 12.

764 **(c) Over-expression of Serrate (Ser) at the Medullary Zone provokes an increase in Crystal**  
765 **Cell numbers and a reduction in Plasmatocyte differentiation.** Pictures show Plasmatocytes  
766 (red, P1 staining) and Crystal Cells (cyan, ProPO staining) in control lymph glands (upper  
767 panels) and in lymph glands with *dome*MESO-Gal4 driven Ser over-expression (middle panels).  
768 Whole Z-project confocal images of primary lobes from wandering third instar larvae are  
769 shown. Scale bar, 20  $\mu$ m. Lower panels: Quantification of the results (\*\*p < 0.001). Error bars  
770 represent SD. *Dome* >, n = 12; *dome* > Ser, n = 12.

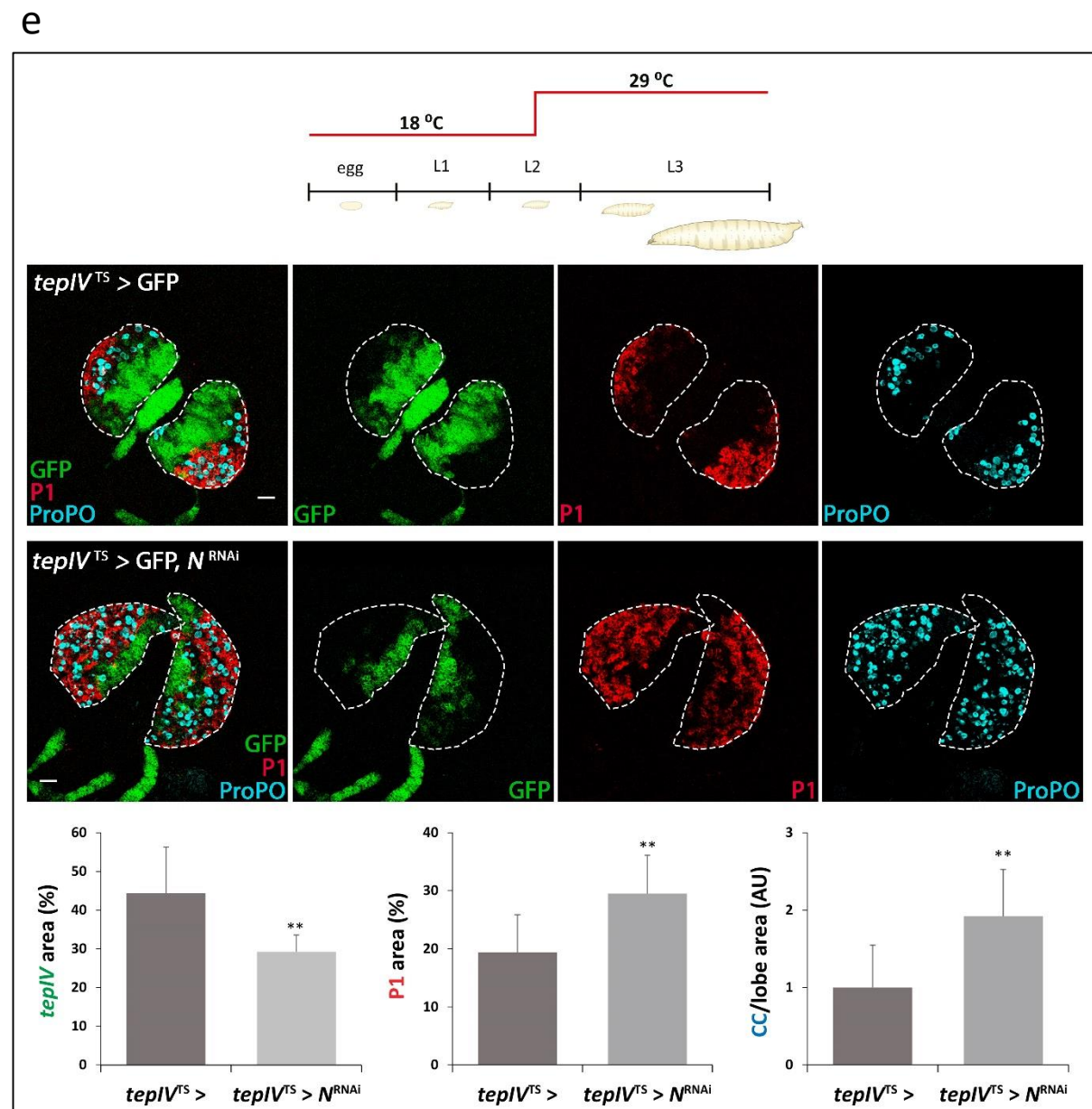
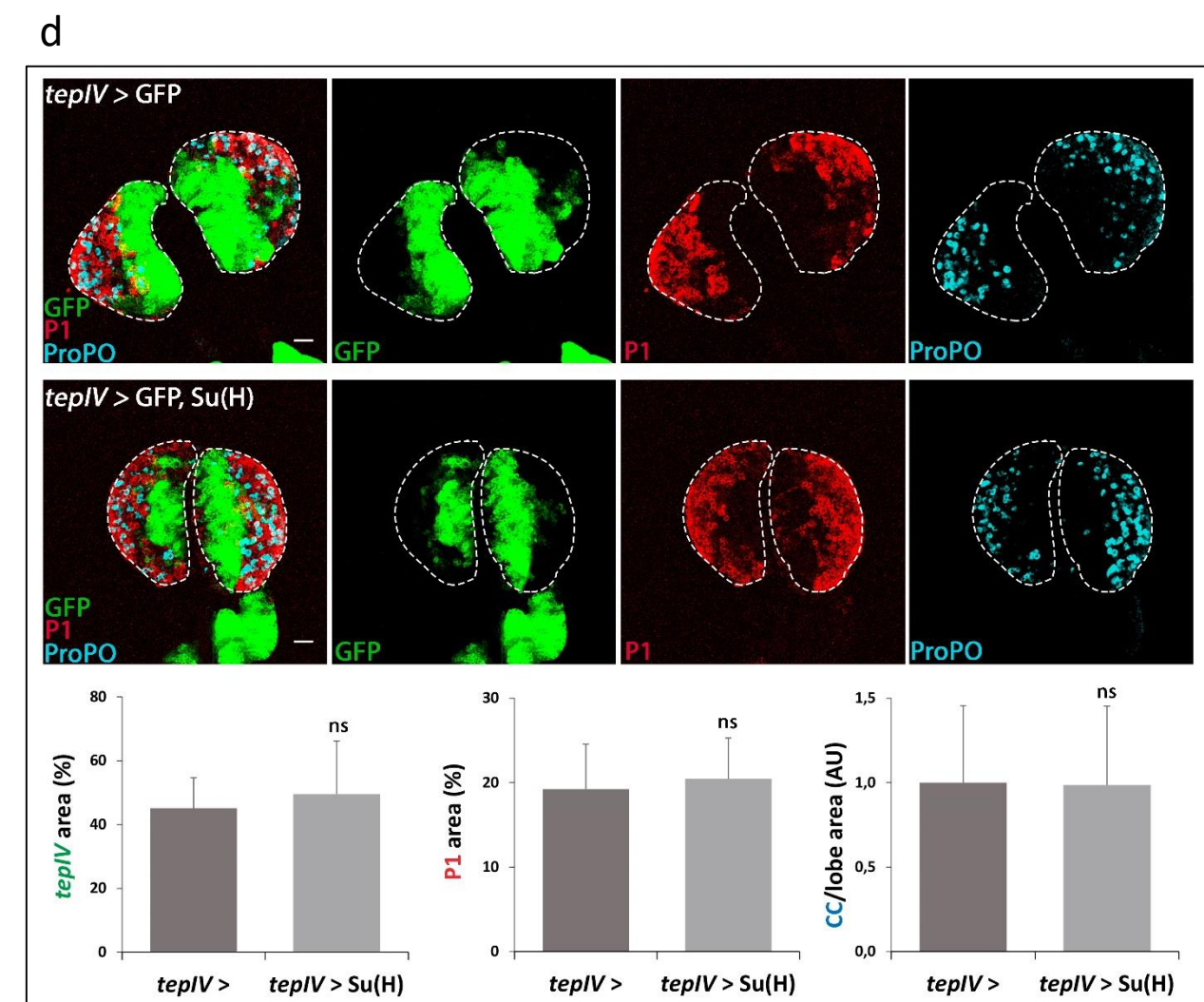
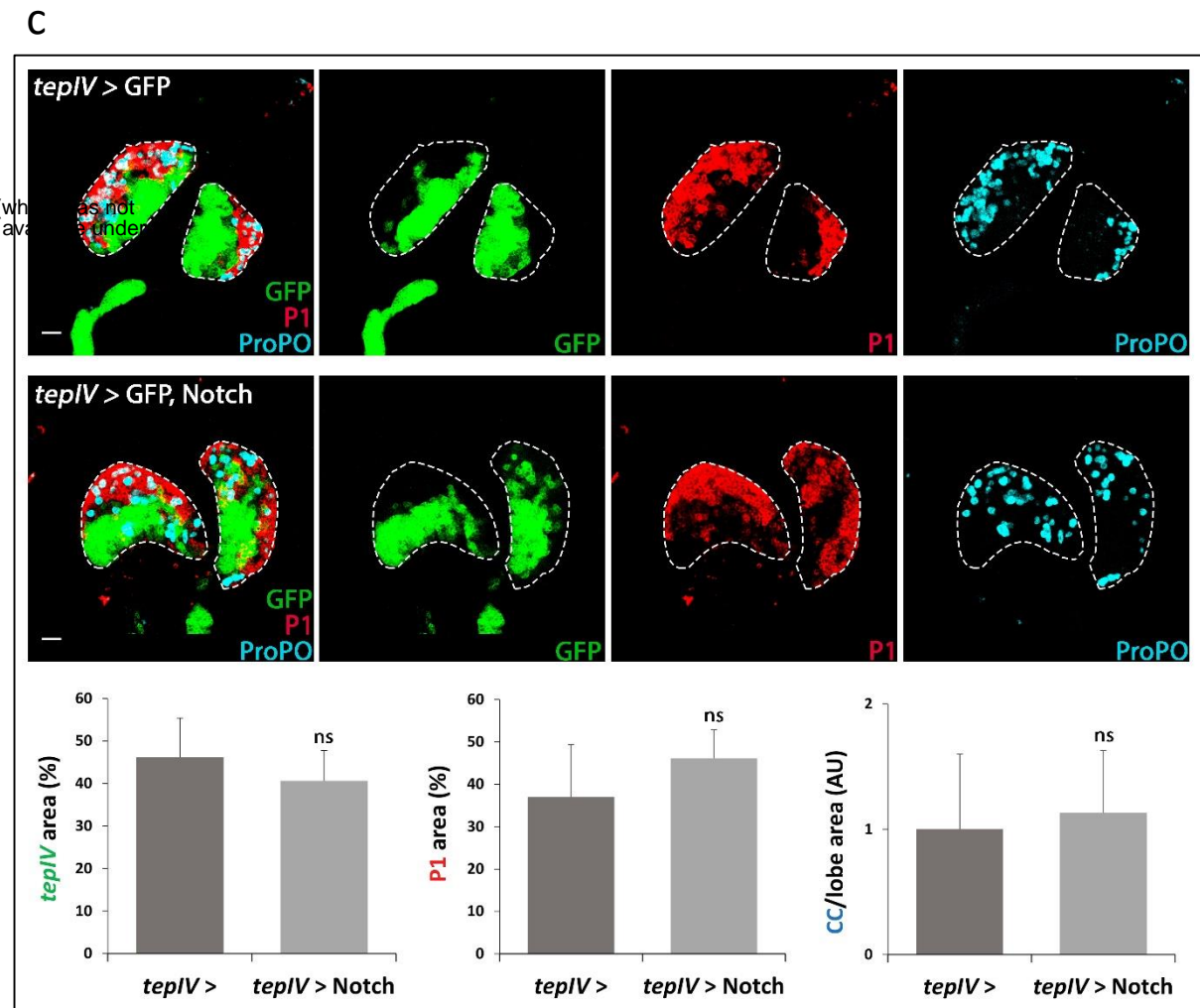
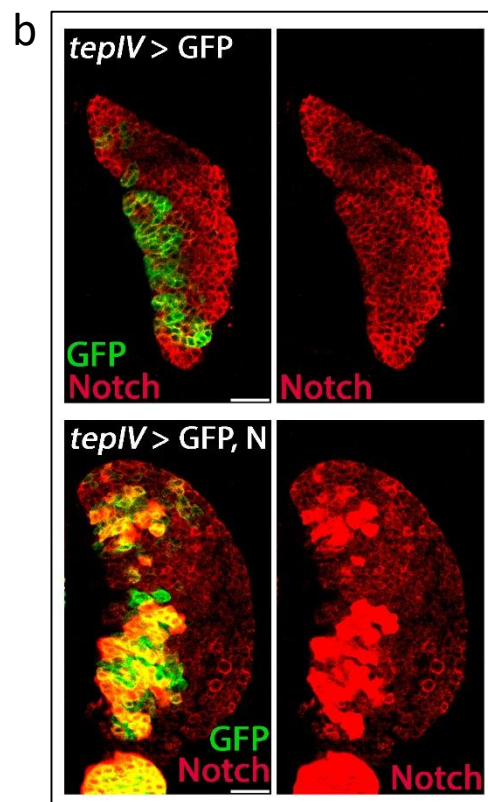
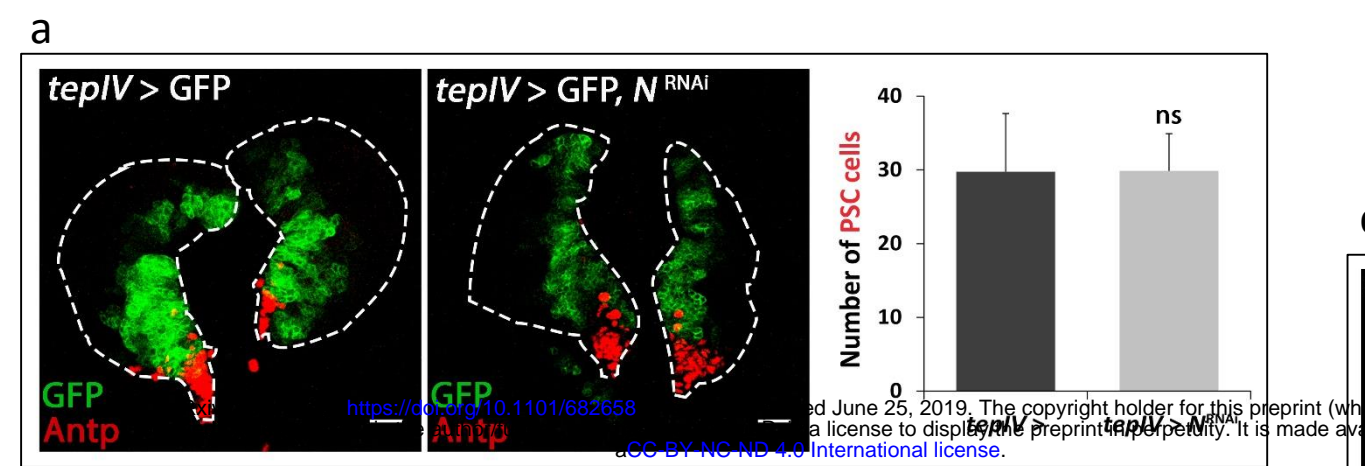
771 **(d) Neuralized (Neu) at the Medullary Zone is required for Crystal Cell differentiation and**  
772 **Plasmatocyte fate inhibition.** Plasmatocytes (red, P1 staining) and Crystal Cells (cyan, ProPO  
773 staining) is shown in control lymph glands (upper panels) and in lymph glands with *neu* RNAi  
774 (*neu*<sup>RNAi</sup>) expression under *dome*MESO-Gal4 driver control (middle panels). Whole Z-project  
775 confocal images of primary lobes from wandering third instar larvae are shown. Scale bar, 20  
776  $\mu$ m. Lower panels: Quantification of the indicated markers (\*\*p < 0.001). Error bars represent  
777 SD. *Dome* >, n = 10; *dome* > *neu*<sup>RNAi</sup>, n = 10.

778

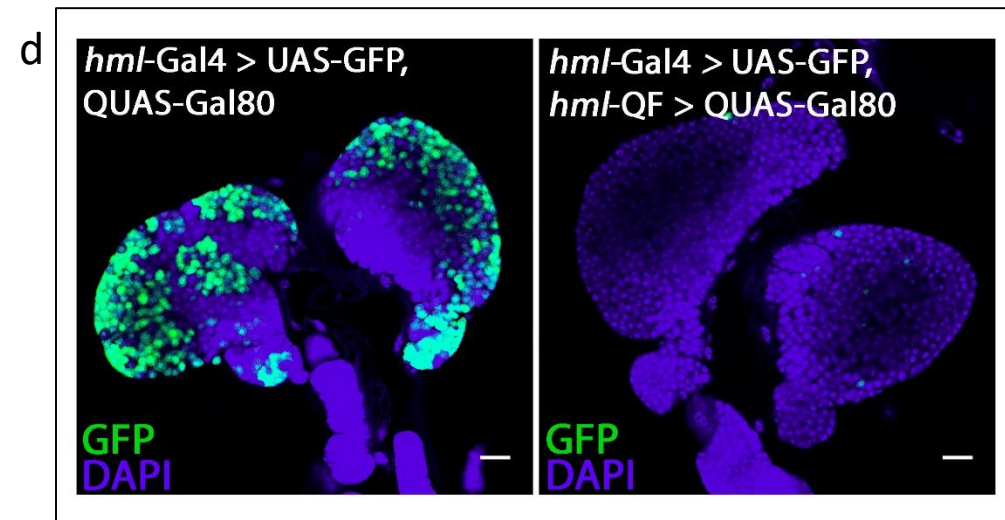
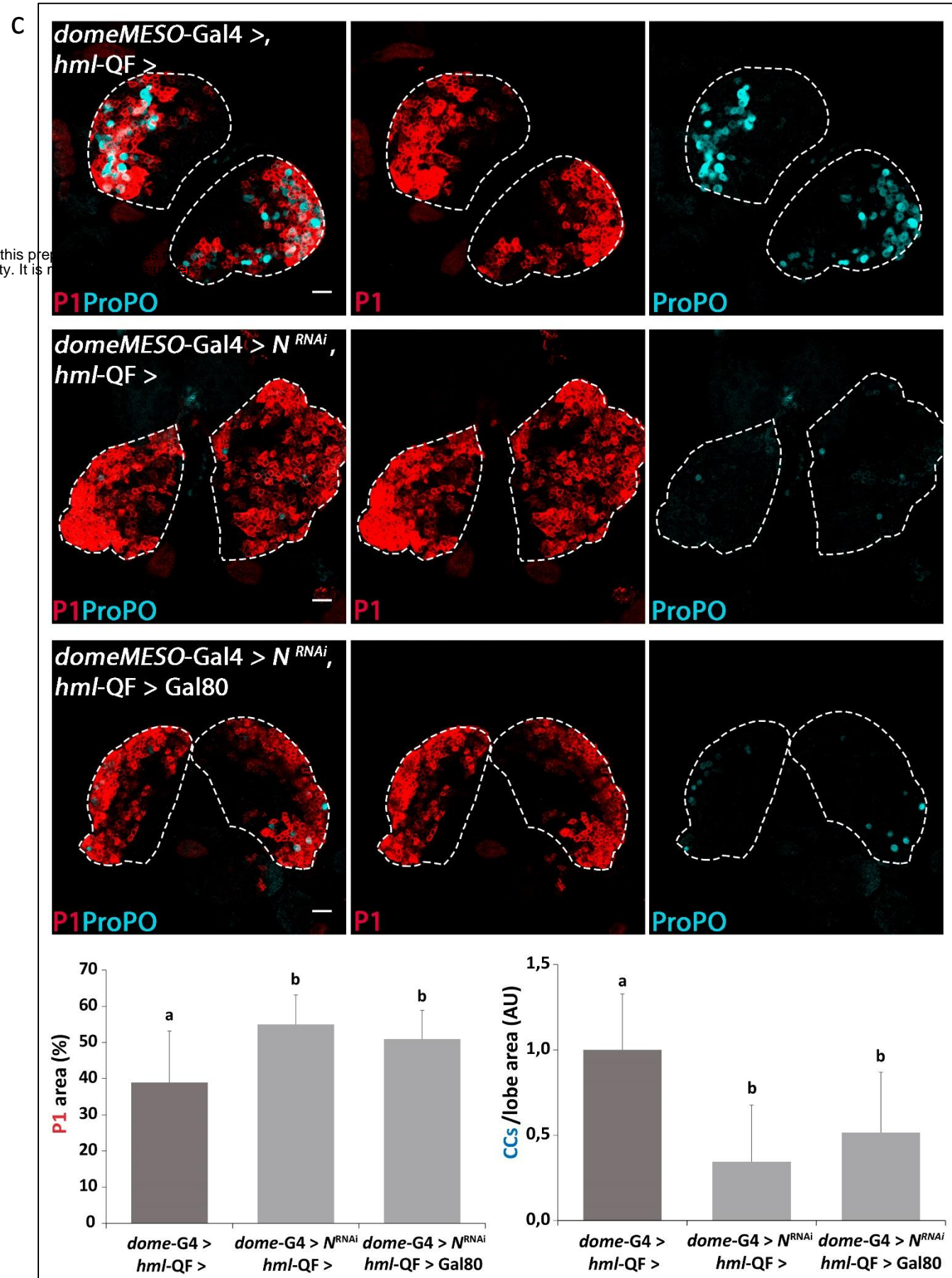
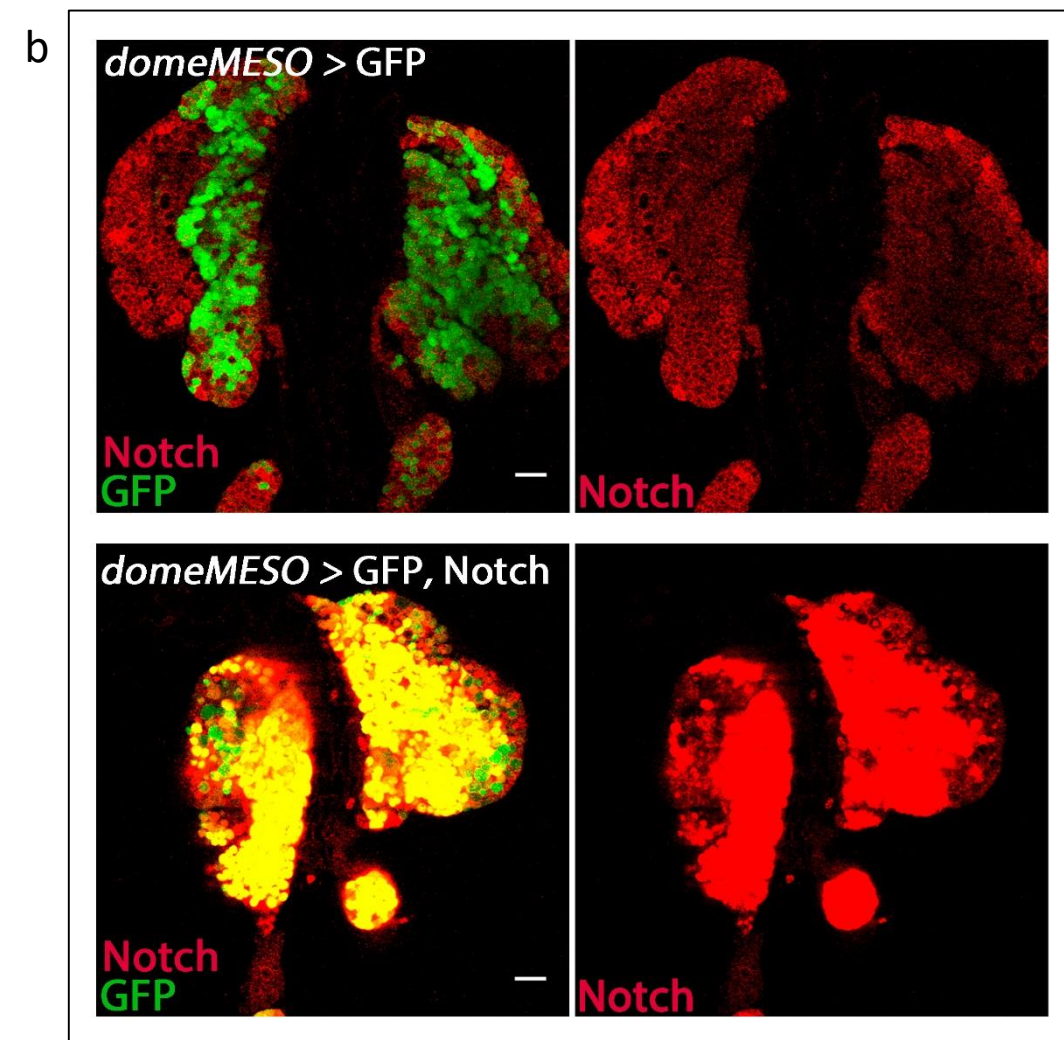
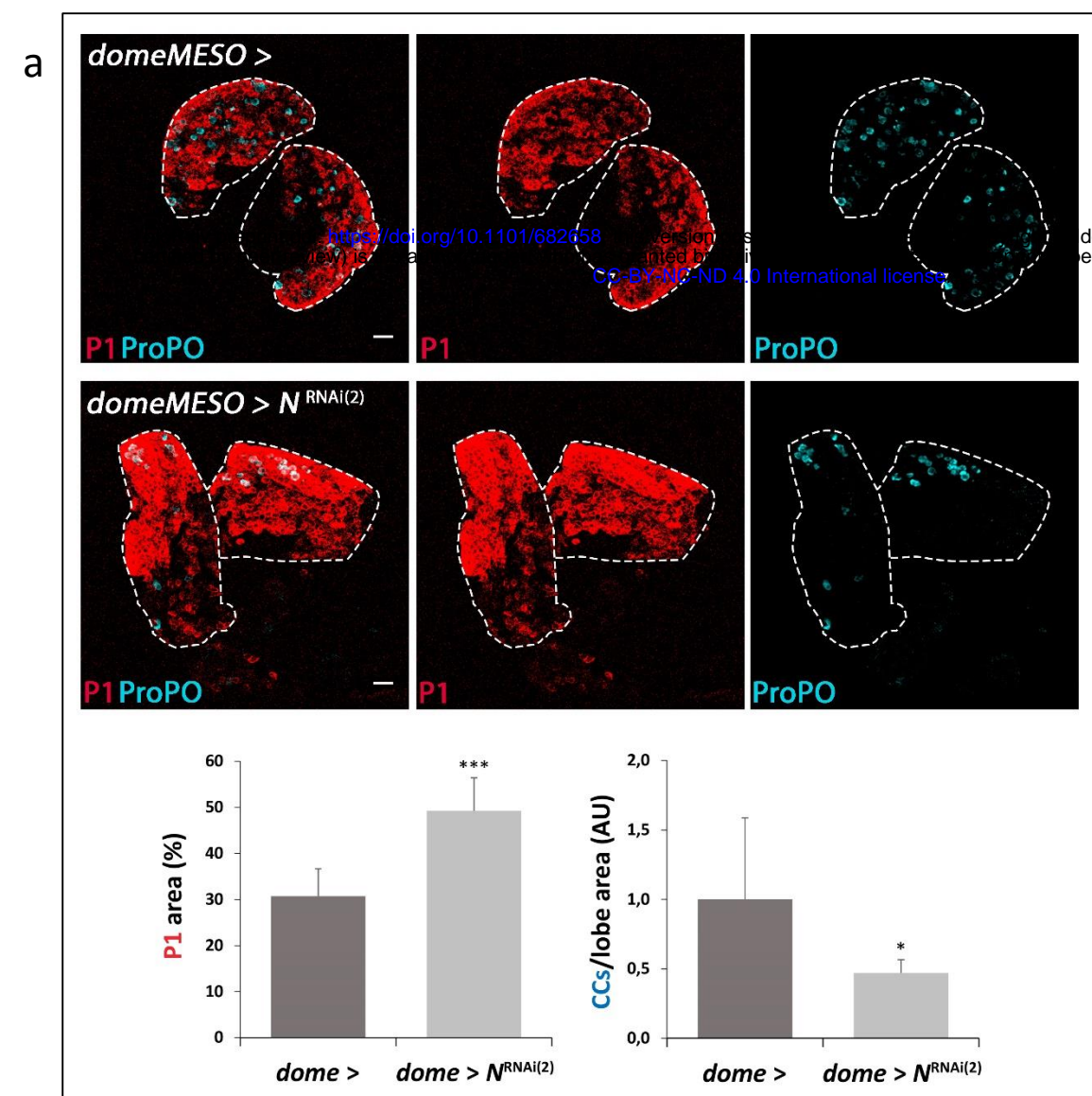
779

780 **Figure 7. Model showing the redefinition of progenitor populations and the functions of the**  
781 **Notch pathway.** In *teplV*<sup>+</sup>, *dome*<sup>+</sup> Core Progenitors (dark green) Notch is activated by its ligand  
782 Ser (Ser), expressed at Posterior Signaling Center (PSC) cells. This Notch activation is required  
783 to avoid premature Core Progenitor differentiation towards both the Plasmatocyte (PL) and  
784 Crystal Cell fate (CC) (upper and lower rows of cells, respectively). Thereafter *teplV* expression  
785 ceases, while *dome* expression continues, defining a second population of progenitors, the  
786 Distal Progenitors (light green). Early Distal Progenitors do not express any differentiation  
787 marker, and constitute the stage where a cell fate decision between the Plasmatocyte and the  
788 Crystal Cell fate is made. This cell fate decision also depends on Notch, which is activated by  
789 Ser expressed at the MZ/CZ boundary. Notch activation in Distal Progenitors induces CC  
790 differentiation and inhibits the PL fate. Without contact from Ser-expressing cells, Distal  
791 Progenitors follow a default PL differentiation program. This early fate decision is evidenced  
792 later in development by the expression of *dome* and *eater* in Distal Progenitors destined to a  
793 PL fate (*eater* expression is represented with a dark red outline), while Distal Progenitors  
794 destined to CCs lack *eater* expression. Once blood cells start expressing *hemolectin* at the  
795 Cortical Zone (*hml*, pink), they are already committed either to a PL or to a CC fate. Cells  
796 committed to a PL fate continue expressing *eater*, while cells committed to become CCs now  
797 express Lozenge (Lz, light blue). Finally, mature PLs co-express *eater*, *hml* and the P1-antigen  
798 (red); while mature CCs co-express Lz and ProPO (dark blue) but have ended *hml* expression.

# Supplementary Figure 1



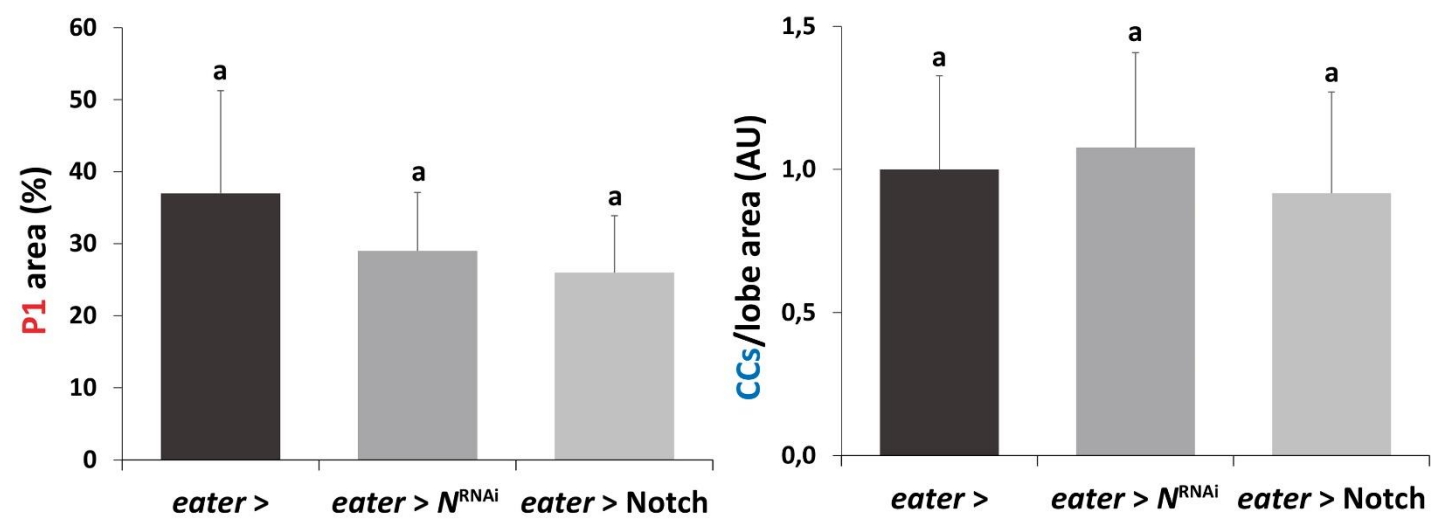
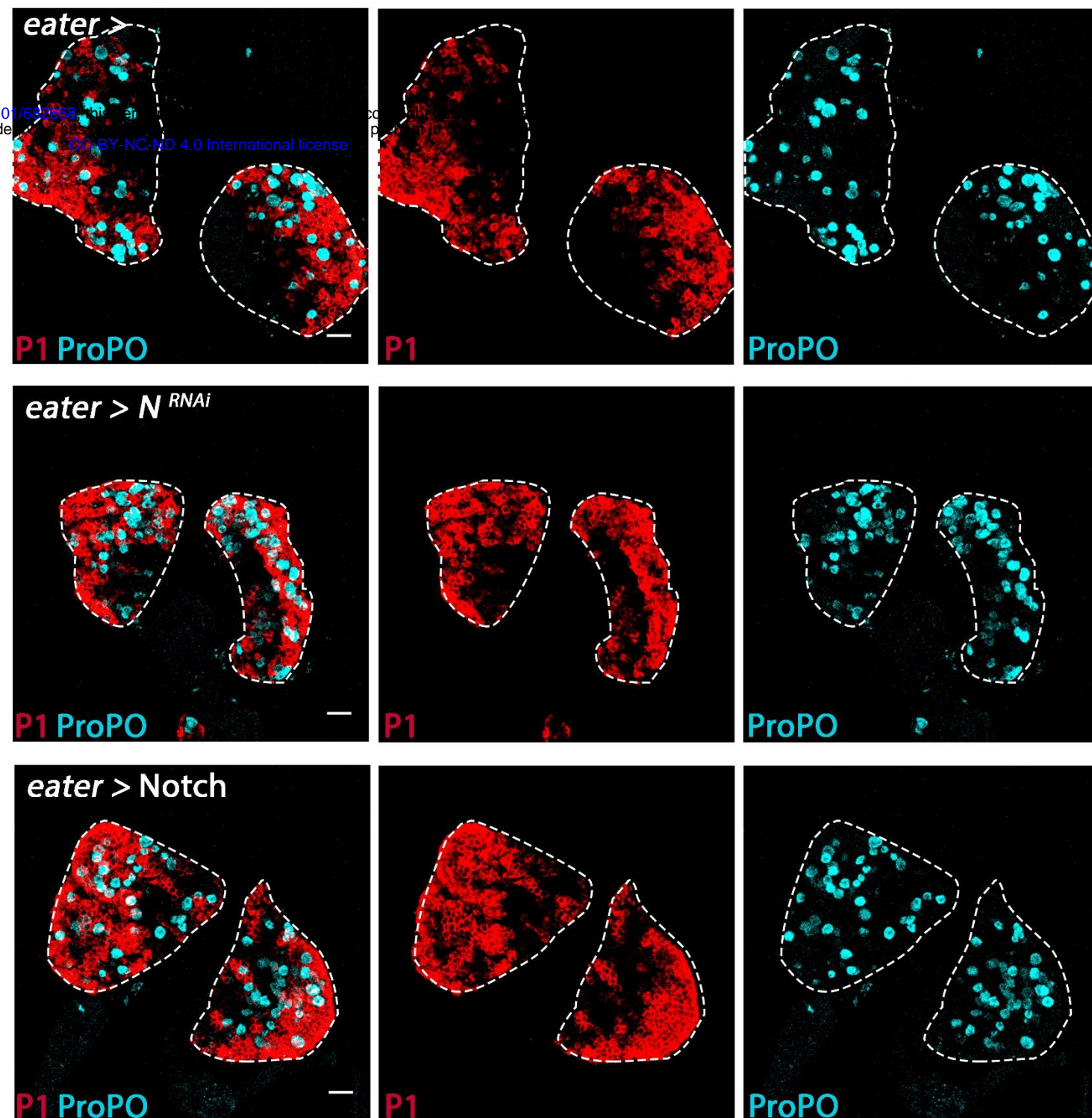
# Supplementary Figure 2



# Supplementary Figure 3

a

bioRxiv preprint doi: <https://doi.org/10.1101/682658>; this version posted August 1, 2020. The copyright holder for this preprint (which was not certified by peer review) is the author/funder, who has granted bioRxiv a license to display the preprint in perpetuity. It is made available under aCC-BY-NC-ND 4.0 International license.





## 800 **Supplementary Figure Legends**

### 801 **Figure S1.**

802 **(a) Notch silencing in Core Progenitors does not affect the size of the Posterior Signaling**  
803 **Center.** *teplV*-Gal4 driven expression of a *notch* RNAi ( $N^{RNAi}$ ), does not affect the number of  
804 Posterior Signaling Center cells, as shown by an anti-Antennapedia (Antp) staining (red). *teplV*  
805 > GFP expression (green) labels Core Progenitors. Left panel: Control lymph gland without RNAi  
806 expression; central panel: Lymph gland that expresses  $N^{RNAi}$  driven by *teplV*-Gal4. Single-plane  
807 confocal images of primary lobes from wandering third instar larvae are shown. Scale bars, 20  
808  $\mu$ m. Right panel: Quantification of the number of Posterior Signaling Center cells per lobe (ns:  
809 Non-significant). Error bars represent SD. *teplV* >, n = 8; *teplV* >  $N^{RNAi}$ , n = 8.

810 **(b) Notch over-expression in Core Progenitors.** Anti-Notch (N) staining (red) was utilized to  
811 demonstrate an increase of Notch levels in Core Progenitors following *teplV*-Gal4 driven over-  
812 expression of full-length Notch. Core progenitors are visualized in green (*teplV* > GFP). Upper  
813 panel: Control lymph glands; lower panel: lymph glands that over-express Notch. Single-plane  
814 confocal images of primary lobes from wandering third instar larvae are shown. Scale bars, 20  
815  $\mu$ m.

816 **(c-d) Over-expression of Notch (d) or Suppressor of Hairless (e) in Core Progenitors has no**  
817 **effect on cell differentiation.** Core Progenitors are visualized in green (*teplV* > GFP);  
818 Plasmatocytes in red (P1 staining); and Crystal Cells in cyan (ProPO staining). Upper panels:  
819 Control lymph glands; middle panels: Lymph glands with *teplV*-Gal4 driven over-expression of  
820 full-length Notch (d) or Su(H) (e). Whole Z-projection confocal images of primary lobes from  
821 wandering third instar larvae are shown. Scale bar, 20  $\mu$ m. Lower panels: Quantification of the  
822 results (ns: Non-significant). Error bars represent SD. *teplV* >, n = 8; *teplV* > Notch, n = 8; *teplV*  
823 > Su(H), n = 8.

824 **(e) Notch is not required for Core Progenitor maintenance at L1 larval stage.** *Notch* (N)  
825 silencing was induced in Core Progenitors from mid L2 stage onwards using the *tub*-Gal80<sup>ts</sup>,  
826 *teplV*-Gal4 genetic combination (*teplV*<sup>TS</sup>), leading to Core Progenitor loss (green: *teplV* > GFP),  
827 and enhanced differentiation of Plasmatocytes (red: P1 staining) and Crystal Cells (cyan: ProPO  
828 staining). Top: temperature protocol utilized in the experiment. Upper panels: control lymph  
829 glands without RNAi expression; middle panels: Lymph glands expressing  $N^{RNAi}$ . Whole Z-  
830 projection confocal images of wandering third instar larvae are shown. Scale bars, 20  $\mu$ m.  
831 Lower panels: Quantification of the results (\*\*p < 0.01). Error bars represent SD. *teplV*<sup>TS</sup>>, n =  
832 9; *teplV*<sup>TS</sup>> $N^{RNAi}$ , n = 10.

833

### 834 **Figure S2.**

835 **(a) Notch silencing with the domeMESO-Gal4 driver, utilizing an alternative notch RNAi**  
836 **construct ( $N^{RNAi(2)}$ ), also provoked increase of Plasmatocytes and reduction of Crystal Cells.**  
837 Plasmatocytes are visualized in red (P1 staining) and Crystal Cells in cyan (ProPO staining).  
838 Upper panels: Control lymph glands; middle panels: Lymph glands with expression of a  $N^{RNAi(2)}$   
839 construct with a different target sequence than the  $N^{RNAi}$  used in Fig. 4a. Whole Z-projection  
840 confocal images of primary lobes from wandering third instar larvae are shown. Scale bar, 20  
841  $\mu$ m. Lower panels: Quantification of the results (\*p < 0.05, \*\*\*p < 0.001). Error bars represent  
842 SD. *dome* >, n = 8; *dome* >  $N^{RNAi(2)}$ , n = 5.

843 **(b) Notch over-expression in domeMESO-positive progenitors.** Anti-Notch (N) staining (red)  
844 was utilized to demonstrate an increase of Notch levels in progenitors (visualized in green;  
845 *domeMESO* > GFP) following *domeMESO*-Gal4 driven over-expression of full-length Notch.

846 Upper panel: Control lymph glands; lower panel: lymph glands that over-express Notch. Single-  
847 plane confocal images of primary lobes from wandering third instar larvae are shown. Scale  
848 bars, 20  $\mu$ m.

849 **(c) *Notch* silencing in *domeMESO*-positive progenitors which do not express *hemolectin (hml)***  
850 **recapitulates increase of Plasmatocytes and reduction of Crystal Cells.** *Notch* RNAi ( $N^{RNAi}$ ) was  
851 expressed with the *domeMESO*-Gal4 driver, together or not with the Gal4 inhibitor Gal80 in  
852 *hml*-positive cells (achieved through *hml*-QF driven expression of QUAS-Gal80). Plasmatocytes  
853 are visualized in red (P1 staining) and Crystal Cells in cyan (ProPO staining). Upper panels:  
854 control lymph glands not expressing  $N^{RNAi}$ ; 2<sup>nd</sup> row panels: lymph glands expressing  $N^{RNAi}$ ,  
855 without Gal80 expression; 3<sup>rd</sup> row panels: lymph glands expressing  $N^{RNAi}$ , with Gal80 expression  
856 in *hml*-positive cells. Whole Z-projection confocal images of primary lobes from wandering  
857 third instar larvae are shown. Scale bar, 20  $\mu$ m. Lower panels: Quantification of the indicated  
858 markers. The letters indicate statistical difference (Tukey's multiple comparison test). Error  
859 bars represent SD. *Dome-G4* >, *hml*-QF >, n = 10; *dome-G4* >  $N^{RNAi}$ , *hml*-QF >, n = 10; *dome-G4*  
860 >  $N^{RNAi}$ , *hml*-QF > Gal80, n = 14.

861 **(d) *Hml*-QF driven expression of QUAS-Gal80 is effective in repressing Gal4 activity at the**  
862 **Cortical Zone.** Gal80 is effective in inhibiting Gal4 activity, as assessed by a virtual block of *hml*-  
863 Gal4 driven UAS-GFP expression (green) when Gal80 is expressed in the same cells using *hml*-  
864 QF > QUAS-Gal80 (right panel). Left panel: control lymph glands without expression of Gal80.  
865 DAPI staining shows nuclei. Single-plane confocal images of wandering third instar primary  
866 lymph gland lobes are shown. Scale bars, 20  $\mu$ m.

867  
868

### 869 **Figure S3.**

870 **(a) Notch does not affect Plasmatocyte or Crystal Cell differentiation after *eater* expression is**  
871 **initiated.** Pictures show expression of the Plasmatocyte marker P1 (red) and the Crystal Cell  
872 marker ProPO (cyan) in control lymph glands (upper panels) and in lymph glands with *eater*-  
873 Gal4 driven expression of *notch* RNAi (2<sup>nd</sup> row panels) or full-length Notch (3<sup>rd</sup> row panels).  
874 Whole Z-projection confocal images of primary lobes from wandering third instar larvae are  
875 depicted. Scale bar, 20  $\mu$ m. Lower panels: Quantification of the indicated markers. Same letter  
876 indicates no statistical difference between means (Tukey's multiple comparison test). *Eater* >,  
877 n = 8; *eater* >  $N^{RNAi}$ , n = 10; *eater* > Notch, n = 10.